

EUMETSAT/ECMWF Fellowship Programme
Research Report No. 41

Atmospheric Motion Vector observations in the ECMWF system: Fifth year report

K. Salonen and N. Bormann

April 2016

Series: EUMETSAT/ECMWF Fellowship Programme Research Reports

A full list of ECMWF Publications can be found on our web site under:

<http://www.ecmwf.int/en/research/publications>

Contact: library@ecmwf.int

©Copyright 2016

European Centre for Medium Range Weather Forecasts
Shinfield Park, Reading, RG2 9AX, England

Literary and scientific copyrights belong to ECMWF and are reserved in all countries. This publication is not to be reprinted or translated in whole or in part without the written permission of the Director-General. Appropriate non-commercial use will normally be granted under the condition that reference is made to ECMWF.

The information within this publication is given in good faith and considered to be true, but ECMWF accepts no liability for error, omission and for loss or damage arising from its use.

Contents

1	Executive summary	2
2	Upcoming changes in the geographical data selection	3
3	Closing the gap between GEO and LEO AMVs with single and dual Metop-A,B AMVs	7
3.1	Metop-A,B AMV quality and characteristics	7
3.2	Experiment setup	9
3.3	Impact assessment	12
3.4	Discussion	12
4	Preparing for the arrival of GOES-R AMVs	18
5	Investigations on accounting for the systematic height assignment errors for AMVs in NWP	26
5.1	Estimating systematic height errors	26
5.2	Comparison of the methods	27
5.3	Results from preliminary impact assessment	29
5.4	Conclusions	31

1 Executive summary

Atmospheric Motion Vector (AMV) observations are assimilated operationally in the European Centre for Medium-Range Weather Forecasts (ECMWF) 4D-Var system from five geostationary (GEO: Meteosat-7, Meteosat-10, GOES-13, GOES-15, MTSAT-2) and four polar orbiting (LEO: Aqua, NOAA-15, NOAA-18, NOAA-19) satellites. Quality and characteristics of AMVs are continuously investigated with the aim of enhancing and improving the use of new and existing AMVs. Table 1 summarises the monitored and used AMVs in the ECMWF system in December 2015.

2015 has been a data rich year with introduction of several new AMV data sets to the operational ECMWF monitoring. China's geostationary satellite FY-2G replaced FY-2E at 105°E on 3rd June 2015. FY-2E was relocated to 86°E and replaced FY-2D on 1st July 2015 when FY-2D retired from operations. Currently FY-2E and FY-2G are operationally passively monitored in the ECMWF system. Completely new geostationary AMVs added to the passive monitoring are the India Meteorological Department (IMD) operated INSAT-3D and the Korean COMS AMVs. Preparations for the satellite changeover from Japan Meteorological Agency (JMA) geostationary satellite MTSAT-2 to Himawari-8 are ongoing. Himawari-8 has also been added to the passive monitoring as well as the NOAA/NESDIS processed VIIRS polar AMVs from the Suomi NPP satellite. VIIRS AMVs are the first operational AMVs processed with the new GOES-R wind algorithm applying nested tracking. A new operational EUMETSAT AMV product is the dual Metop-A,B AMVs with global coverage.

The geographical data selection applied in the data assimilation process has been revised for the upcoming ECMWF integrated forecasting system (IFS) cycle 41r2 and the results are discussed in Section 2. The main change is to extend the accepted satellite zenith angle from 60° to 64° for AMVs from geostationary satellites. This change reduces the gap between the coverage of geostationary and polar AMVs. Data assimilation experiments indicate neutral to slightly positive impact from the changes.

The impact of using EUMETSAT-processed AVHRR AMVs from Metop-A and Metop-B has been investigated in order to further reduce the gap in AMV coverage and the results are presented in Section 3. EUMETSAT has introduced several changes to the polar AMV processing during recent years and the long term monitoring statistics indicate improvements in the data quality. EUMETSAT has also made available a new dual Metop-A,B AMV product. It is the first AMV product with global coverage. At high latitudes the dual Metop AMVs have similar characteristics to the single Metop AMVs. In the tropics the dual Metop AMVs have high biases and thus using the data equator-wards of 40°N/S is currently not considered. Data assimilation experiments indicate positive impact on short range and neutral impact on longer range forecasts when Metop AMVs are used. Operational assimilation of these additional AMVs started on 4th February 2016.

Section 4 summarises the work done so far in preparation for the use of GOES-R AMVs. A proxy dataset provided by NOAA/NESDIS has been evaluated that uses the new nested tracking AMV algorithm that will be used to derive AMVs from GOES-R. This new algorithm provides several new parameters giving information about the characteristics of the cluster used in the AMV tracking as well as uncertainties in the height assignment process. The results obtained in the ECMWF system have been compared to those of the University of Wisconsin-Madison/Cooperative Institute for Meteorological Satellite Studies (CIMSS) in the framework of the GOES-R Visiting Scientist Program. The first results indicate that the new parameters have great potential to be used in the AMV quality control or observation error specification in the future.

Work on characterising systematic height assignment errors for AMVs has continued and a status update is given in Section 5. Previous work estimated these from long-term model best-fit pressure statistics. An alternative estimate for systematic height assignment errors can be derived from space-borne lidars which provide independent cloud height information. The similarities and differences of the two systematic height assignment error estimates have been investigated in co-operation with the Hans-Ertel-Centre for Weather Research. Overall the results from the two approaches share many similar characteristics. The comparison gives further

Table 1: Overview of the use of AMV data in the ECMWF system in December 2015.

	IR	Cloudy WV	Clear WV	VIS
Meteosat-7	used	used	monitored	used
Meteosat-10	used	used	monitored	used
GOES-13	used	used	monitored	used
GOES-15	used	used	monitored	used
MTSAT-2	used	used	monitored	used
Himawari-8	monitored	monitored	monitored	monitored
CMA FY-2E	monitored	monitored	monitored	-
CMA FY-2G	monitored	monitored	monitored	-
IMD INSAT-3D	monitored	monitored	monitored	monitored
COMS	monitored	monitored	monitored	monitored
MODIS AMVs from Aqua	used	used	used	-
MODIS AMVs from Terra	monitored	monitored	monitored	-
AVHRR AMVs from NOAA-15, -18 and -19	used	-	-	-
AVHRR AMVs from METOP-A, METOP-B and dual METOP-A,B	monitored	-	-	-
VIIRS AMVs from Suomi NPP	monitored	-	-	-

confidence in the estimates of the systematic errors. Preliminary data assimilation experiments have been performed with the ECMWF system. The AMV heights are re-assigned based on the best-fit pressure statistics from the lidar comparison period. The observation fit statistics give somewhat mixed results. Generally the fit of AMVs to the model background has slightly degraded while the fit of other wind observations has slightly improved as a consequence of re-assigning the AMV heights. The forecast scores indicate neutral to slightly positive impact. The results are encouraging but further investigations are required.

2 Upcoming changes in the geographical data selection

The geographical data selection applied in the data assimilation process, commonly referred to as blacklisting, has been revised for AMVs for the upcoming ECMWF IFS cycle 41r2 which is expected to be operational in the first quarter of 2016. The work is motivated by several improvements that have been implemented for AMV processing from the data providers side in the past years (e.g. [Borde and Oyama, 2008](#); [Qi et al., 2014](#)). In addition the use of AMVs in the ECMWF system has been significantly advanced by introducing situation dependent observation errors and relaxations to the quality control procedures ([Salonen and Bormann, 2013](#)). However, at that point the blacklisting decisions were kept unchanged.

Several relaxations to the blacklisting have been tested with the ECMWF IFS cycle 40r2 at T511 resolution, 137 vertical levels, and 12-hour 4D-Var over summer (2.8-31.10.2013) and winter (1.1-31.3.2014) periods. All operationally assimilated conventional and satellite observations were used in the experiments.

The main change is to extend the accepted satellite zenith angle from 60° to 64° for AMVs from geostationary satellites. This will help to reduce the gap between the coverage of geostationary and polar AMVs. Extending the accepted satellite zenith angle up to 68° was also tested. This would allow to use the full disc of available geostationary AMVs but the data assimilation experiments indicated some degradation in the forecast quality

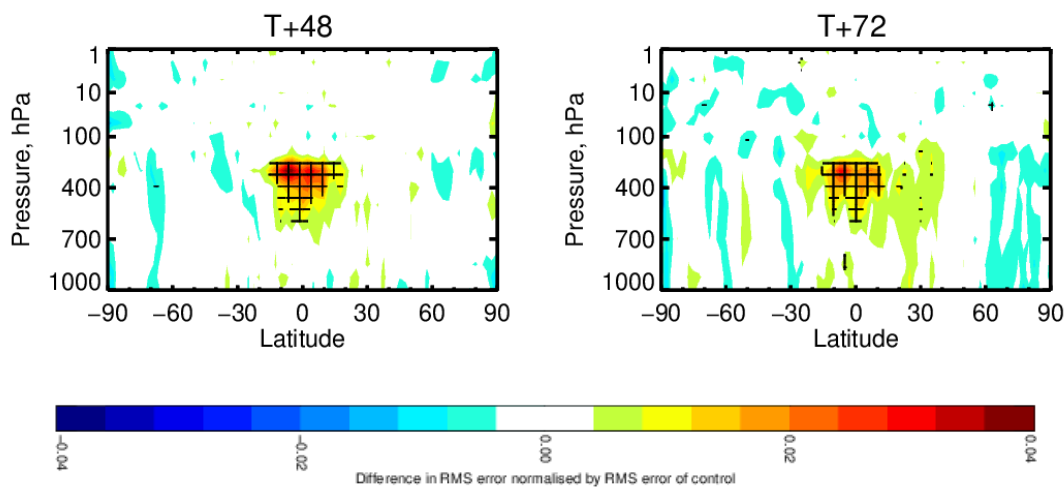


Figure 1: Zonal plots of the normalised difference wind forecast RMS error for 2 and 3 day forecasts for experiment testing relaxed blacklisting for Meteosat-10 AMVs over the tropics. Blue shades indicate positive impact and green and red shades negative impact. The considered periods are 2.8-31.10.2013 and 1.1-31.3.2014.

over southern hemisphere high latitudes. Blacklisting the data over sea-ice did not improve the forecast scores. Thus, a decision to use the limit 64° for the satellite zenith angle has been made.

Blacklisting for Meteosat-10 IR AMVs between 460 - 700 hPa at midlatitudes will also be removed. Monitoring statistics now indicate data quality comparable to heights where AMVs are actively used and experiments indicate neutral forecast impact from using the data.

Relaxing blacklisting decision for high level AMVs over the tropics was also considered with the view that the use of situation dependent observation errors would allow usage of this data. Currently all Meteosat-10 AMVs below 250 hPa height are blacklisted due to positive observation minus background (OmB) bias. However, relaxing the blacklisting decisions over the tropics led to degraded forecast scores. Figure 1 shows the zonal plots of the normalised difference of the wind forecast RMS error for 48-hour and 72-hour forecasts. The verification has been done against each experiment's own analysis. The forecast impact is clearly negative over the tropics and persists through the whole forecast range. Thus, AMVs below 250 hPa in the tropics remain blacklisted.

The relaxations for the blacklisting that will be implemented to the operational IFS cycle 41r2 were tested over summer (1.6-30.9.2014) and winter (1.2-30.4.2014) periods with the ECMWF IFS cycle 41r1 at T639 resolution, 137 vertical levels, and 12-hour 4D-Var. Again, all operationally assimilated conventional and satellite observations were used in the experiments. In the following two experiments are considered:

- **Ctl:** Control experiment applies the current operational blacklisting.
- **Relaxed:** Relaxed blacklisting for AMVs, accepted satellite zenith angle 64° , Meteosat-10 IR AMVs used 460-700 hPa at midlatitudes.

Figure 2 shows a sample coverage of active AMVs on 1st February 2014 12 UTC cycle. The dark grey dots indicate AMVs that are active when the operational blacklisting for AMVs is used and the brown dots indicate the additional AMVs from relaxing the blacklisting decisions. Most of the additional active AMVs are from the edges of the satellite discs as a consequence of the relaxed satellite zenith angle criteria. In general, relaxing

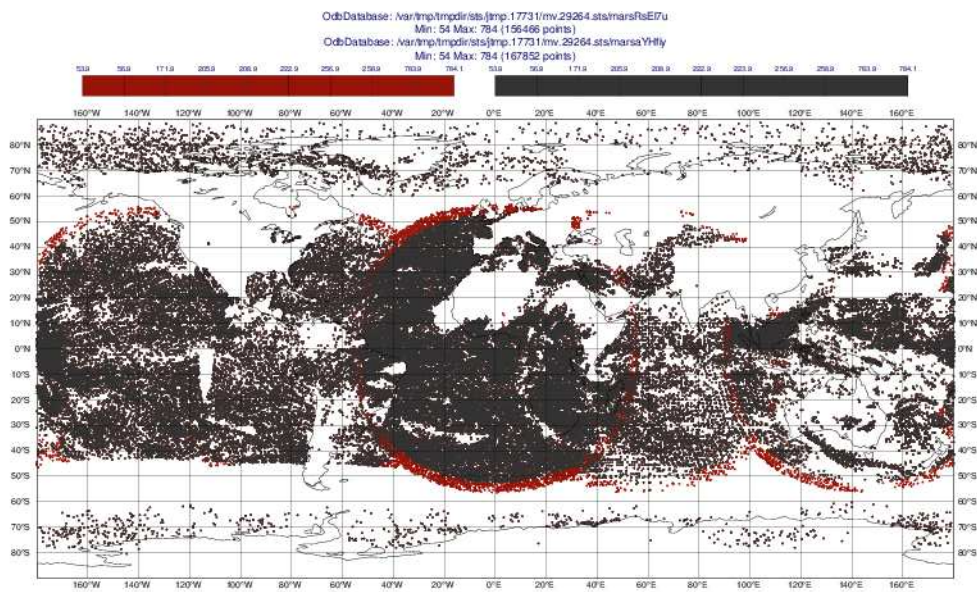


Figure 2: Sample coverage of active AMVs on 1st February 2014 12 UTC cycle. The dark grey dots indicate AMVs that are active when the operational blacklisting for AMVs is used and the brown dots indicate the additional active AMVs from relaxing the blacklisting decisions.

the blacklisting decisions leads to 2 - 18% increase in the use of AMVs depending on height. Relative to the number of previously assimilated AMVs, the change is largest at mid levels where overall not so many AMVs are available.

The 7-month long impact study indicates neutral to positive forecast impact from relaxing the blacklisting decisions. Figure 3 shows zonal plots of the normalised difference of the wind forecast RMS error for different forecasts lengths. The verification has been done against each experiment's own analysis. The main positive impact is seen over the high latitudes.

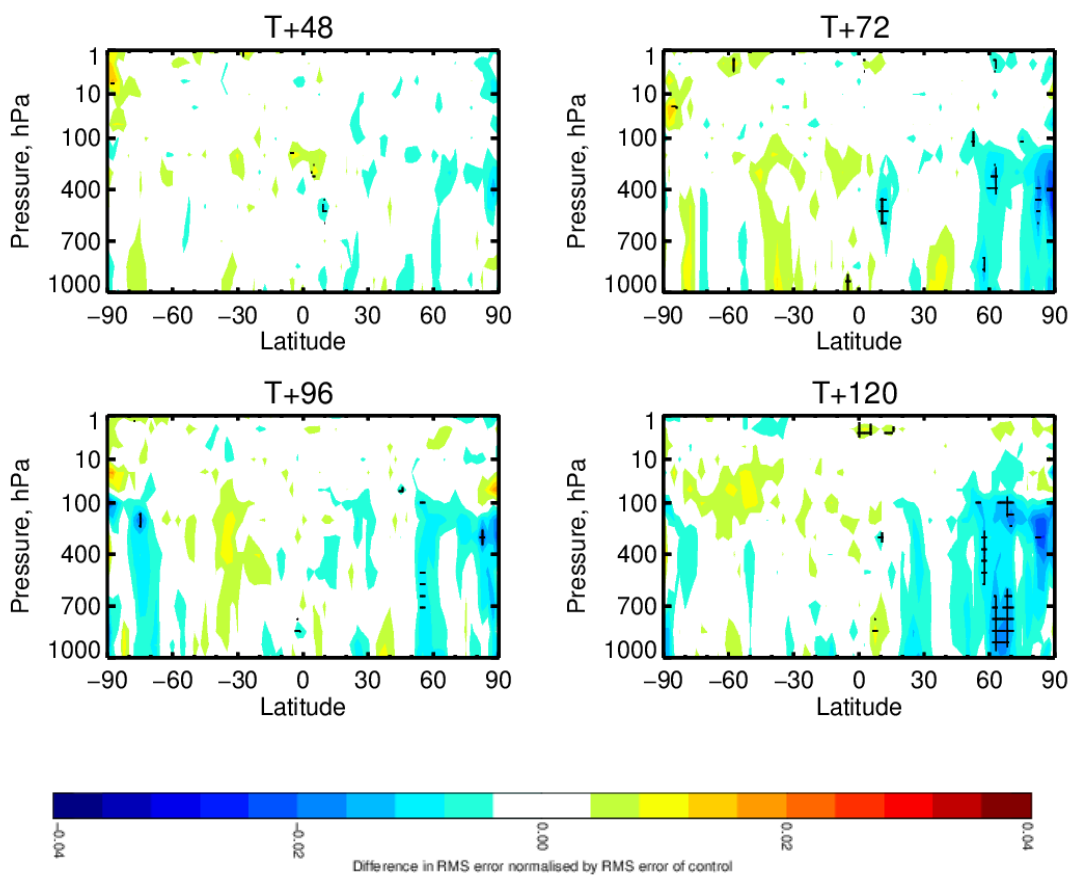


Figure 3: Zonal plots of the normalised difference (**Relaxed - Ctl**) wind forecast RMS error for 2 to 5 day forecasts. Blue shades indicate positive impact and green and red shades negative impact. The considered periods are 1.2-30.4.2014 and 1.6-30.9.2014.

3 Closing the gap between GEO and LEO AMVs with single and dual Metop-A,B AMVs

The spatial coverage of AMVs is generally equatorward of 55-60° latitude for GEO satellites and poleward of 70° latitude for the LEO satellites. Thus, in both hemispheres there is a 10-15° gap in the AMV coverage over the latitudinal zones where the dynamically active polar jet streams are located. The planned blacklist change for the maximum accepted satellite zenith angle, discussed in Section 2, helps to reduce the gap but it will not entirely close it.

AMV providers have actively developed their products in order to close the coverage gap. University of Wisconsin Space Science and Engineering Center (SSEC), the University of Wisconsin Cooperative Institute for Meteorological Satellite Studies (CIMSS) and the National Oceanic and Atmospheric Administration (NOAA) have developed an algorithm to create AMVs from LEO/GEO composites (Lazzarra et al., 2014). Deriving LEO/GEO AMVs is done with a very similar method as for the MODIS, NOAA AVHRR, and GOES AMVs. Three successive images are used to track coherent features and the coverage is polewards from 50° N/S. The LEO/GEO AMVs are used operationally in the Naval Research Laboratory Atmospheric Variational Data Assimilation System Accelerated Representer (NAVDAS-AR) and at the National Center for Atmospheric Research in their Antarctic Mesoscale Prediction System (AMPS) model (Hoover et al., 2012). Also Met Office has been using the data operationally since March 2015 (Warrick, personal communication). LEO/GEO AMVs have not been investigated in the ECMWF system yet. At this point higher priority has been given to single and dual Metop-A,B AMVs as they have better coverage and higher density of observations compared to the LEO/GEO AMVs.

EUMETSAT derives polar AVHRR AMVs from Metop-A and Metop-B satellites. The polar wind processing is based on image pairs. This strategy results in the loss of the temporal consistency test between the two consecutive intermediate vectors usually obtained from image triplets (Borde et al., 2013). However, the major advantages of the approach are that it decreases the tracking time from two orbit periods to one, and it allows extending the coverage up to 45-50° N/S. EUMETSAT has also made available a new dual Metop-A,B AMV product (Hautecoeur et al., 2014). Metop-A and Metop-B are on the same orbital plane and the temporal gap between the two images used for tracking clouds is about 50 minutes. The dual Metop-A,B AMV product has global coverage. Together the single and dual Metop-A,B AMVs provide an excellent coverage over the gap between the currently operationally used LEO and GEO AMVs.

The impact of single and dual Metop-A,B AMVs has been investigated in the ECMWF system and the results are discussed in the following subsections.

3.1 Metop-A,B AMV quality and characteristics

EUMETSAT has significantly improved their polar wind processing during recent years. The latest major updates were introduced into operations in May 2014 and the updates had considerable impact on the AMV characteristics and thus on the monitoring statistics (Salonen and Bormann, 2015). At mid and low levels the changes clearly improved the data quality. The long standing issue with positive speed bias is not present after the update and the magnitude of the speed bias is within $\pm 0.5 \text{ ms}^{-1}$. However, at high levels a negative speed bias up to -2 ms^{-1} is now seen whereas before the changes the bias was close to zero. RMSVD has generally decreased at all levels. Metop-A and Metop-B AMVs share similar characteristics.

Figure 4 shows zonal plots of the OmB wind speed bias (upper panels), RMSVD (middle panels) and number of observations (lower panels) for single Metop-A (left) and dual Metop-A,B AMVs (right). At high latitudes the bias and RMSVD statistics for the dual Metop-A,B AMVs are very similar to the single Metop AMVs. The

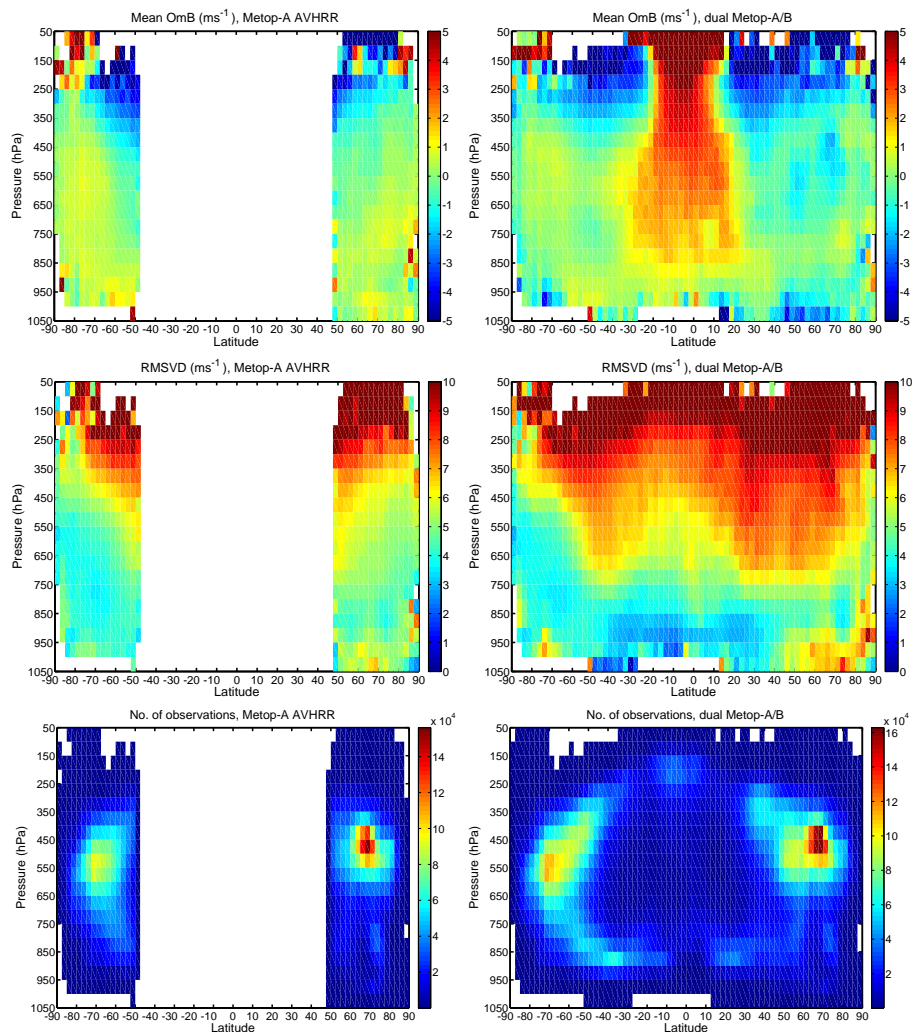


Figure 4: Zonal plots of the OmB wind speed bias (upper panel), RMSVD (middle panel) and number of observations (lower panel) for single Metop-A AMVs (left) and dual Metop-A,B AMVs (right). The forecast independent QI is greater than 60.

dual-Metop AMVs have large positive bias over the tropics, especially above 700 hPa. However, outside the tropics the data indicates promising potential for further investigations.

Figure 5 shows the RMSVD for different forecast independent QI values for single Metop-A AMVs. The considered period is 19th April - 18th May 2015. The magnitude of RMSVD slightly decreases when the QI value increases. However, the dependency is not very strong. EUMETSAT introduced a bug fix to the QI calculation on 19th May 2015. This fix did not have a strong impact on the data characteristics in terms of wind speed bias or RMSVD. Figure 6 shows the same as Fig. 5 but for the period 20th May - 19th June 2015. There are more AMVs assigned with high QI values mainly at mid levels, otherwise the data characteristics are similar to those before the fix. In the following, a threshold of greater than 60 for the forecast independent QI is used. This is the standard NWP SAF QI threshold for polar AMVs and based on Fig. 5 and Fig. 6 looks like a sensible choice for the Metop AMVs.

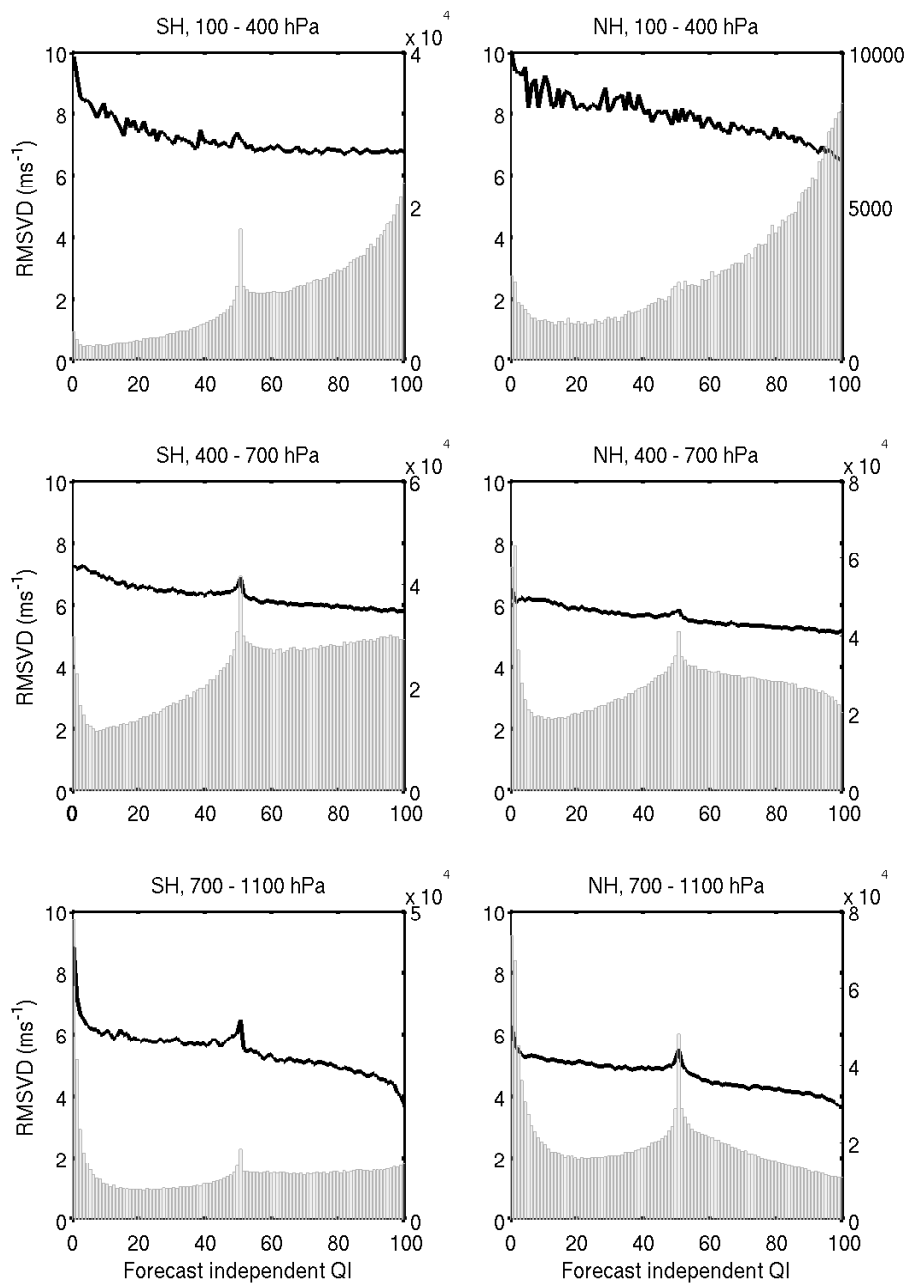


Figure 5: The RMSVD (black line) and number of observations (grey bars) for different QI values at different heights (upper panels 100 - 400 hPa, middle panels 400 - 700 hPa and lower panels 700 - 1100 hPa) for single Metop-A AMVs. Left panels are for southern hemisphere and right panels for northern hemisphere. The considered period is 19th April - 18th May 2015.

3.2 Experiment setup

The impact of using the single Metop-A and Metop-B as well as dual Metop-A,B AVHRR AMVs has been studied over a 6-month long period covering 1st January - 30th June 2015. The ECMWF IFS cycle 41r1 at T639 resolution, 137 vertical levels and 12-hour 4D-Var has been applied in the experiments. The following experiments are discussed here:

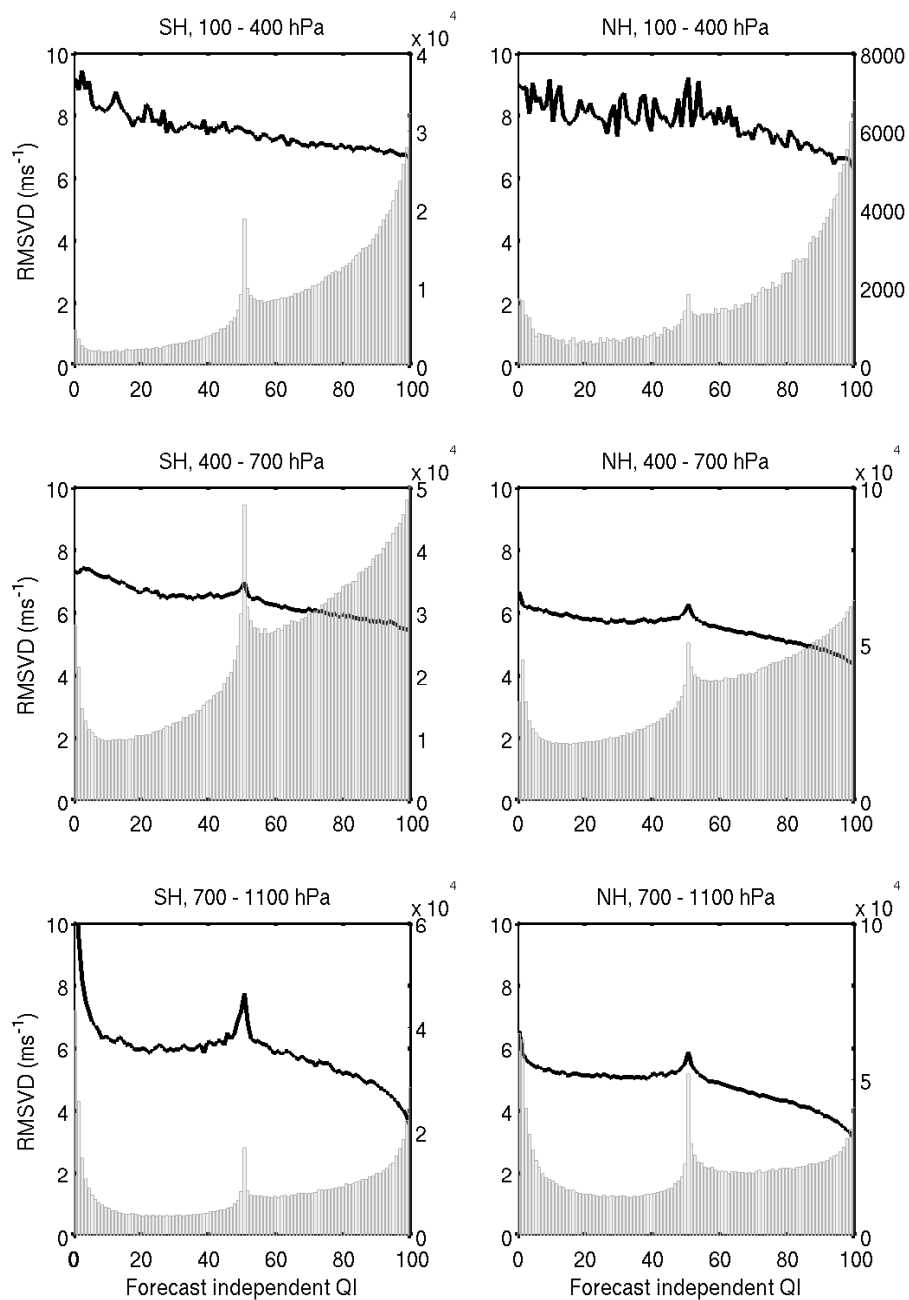


Figure 6: Same as Fig. 5 but for 20th May - 19th June 2015.

- **Ctl**: All operationally assimilated conventional and satellite observations are used. The AMV coverage is similar as in Fig. 2 when the operational blacklisting is used.
- **Single50**: Single Metop-A and Metop-B AMVs with forecast independent QI greater than 60 are used polewards from 50° N/S, on top of the observations used in **Ctl**.
- **Single60_Dual40**: Single Metop-A and Metop-B AMVs with forecast independent QI greater than 60 are used polewards from 60° N/S, and dual Metop AMVs are used between latitudes 40° and 60° over both hemispheres on top of the observations used in **Ctl**. This choice is motivated by the fact that over

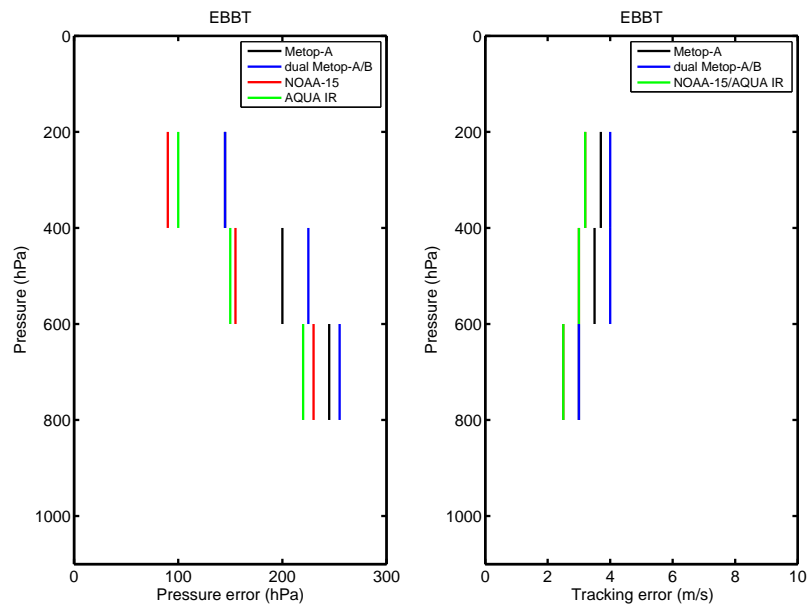


Figure 7: The height error (left panel) and the tracking error estimates (right panel) for Metop-A (black), dual Metop-A,B (blue), NOAA-15 (red) and Aqua IR (green) AMVs.

the polar regions the single Metop AMVs have on average slightly lower RMSVD compared to the dual Metop AMVs and equatorwards 40° N/S geostationary satellites are providing excellent AMV coverage.

Based on the QI statistics (Fig. 5 and Fig. 6) it was decided to use a threshold of greater than 60 for the forecast independent QI in the experiments. For other polar AMVs (MODIS AMVs from Aqua or AVHRR AMVs from NOAA-15,-18,-19 satellites) no QI threshold is used in the ECMWF system as the monitoring statistics do not indicate higher quality for higher QI values. Otherwise the blacklisting decisions for single and dual Metop-A,B AMVs are similar to the AVHRR AMVs from the NOAA satellites. Thus, no AMVs below 400 hPa over land and no AMVs below 700 hPa over sea ice are used.

The ECMWF system uses situation dependent observation errors for AMVs from the IFS cycle 40r1 onwards (Salonen and Bormann, 2013). The height errors are defined based on model best-fit pressure statistics and tracking errors are defined from OmB statistics from cases where the wind error due to height error is small. The left panel of Fig. 7 shows the height errors for Metop-A, dual Metop-A,B, NOAA-15 and Aqua IR AMVs. For the single and dual Metop AMVs the height error estimates vary between 150 and 250 hPa depending on height. The values are somewhat larger than what are used for AVHRR AMVs from NOAA satellites and for IR AMVs from Aqua.

So far, tracking errors have been defined separately only for geostationary and polar AMVs. As the derivation process used at NOAA/NESDIS and at EUMETSAT are different, the tracking errors have been estimated for single and dual Metop AMVs separately. Also the tracking errors for Metop AMVs are somewhat larger than for other polar AMVs, and they are also slightly larger for the dual Metop AMVs compared to the single Metop AMVs. The right panel of Fig. 7 shows the tracking errors used in the experiments. The final observation error for each AMV is calculated following the Forsythe and Saunders (2008) approach.

3.3 Impact assessment

Figure 8 shows a sample coverage of active AMVs on 1st March 2014 12 UTC cycle, upper panel is for **Ctl**, middle panel for **Single50** and lower panel for **Single60_Dual40** experiment, respectively. Active single Metop-A and Metop-B AMVs are marked with brown and dual Metop-A,B AMVs with dark red, all other AMVs are marked with grey. Both **Single50** and **Single60_Dual40** experiments provide a good coverage over the gap where no AMVs are currently used actively in operations. The **Single60_Dual40** experiment is also able to fill the gap over the southern hemisphere where GOES-13 and GOES-15 AMVs are not available due to the chosen scanning strategy.

Figure 9 shows the number of active AMVs in the three considered experiments (right panel) and the relative increase in the used AMVs (left panel). The use of Metop AMVs increases the number of active AMVs from few percent up to over 200% depending on height. The increase is largest at mid levels where typically less AMVs are available than at high and low levels.

Using single and dual Metop-A,B AMVs does not change the mean wind analysis significantly. Thus, no areas where the use of Metop AMVs would weaken or strengthen the mean wind field can be identified. Figure 10 shows the mean wind analysis at 250 hPa (upper panel) for the **Ctl** experiment and the vector difference of the mean wind analysis between the **Ctl** and **Single60_Dual40** experiments (lower panel) for January 2015. The changes in the mean wind analysis are mainly less than $\pm 0.5 \text{ ms}^{-1}$. This is the case at all pressure levels and other time periods as well. Results are similar for the **Single50** experiment.

In general, the observation fit statistics indicate mainly neutral impact from using the single and dual Metop-A,B AMVs. Figure 11 shows the normalised OmB standard deviation for radiosonde wind observations over the Southern polar cap. Values below 100% indicate that the radiosonde observations fit better with the **Ctl** background and values above 100% that with the **Single60_Dual40** background. The differences are within the error bars and thus statistically not significant. Again, the results are very similar for the **Single50** experiment. The fact that the observation fit statistics to other observations do not change significantly suggests that the single and dual Metop-A,B AMVs generally agree with the rest of the observing network.

To investigate the impact of using the single and dual Metop-A,B AMVs on longer range forecasts, verification against each experiment's own analysis has been done. Figure 12 shows the zonal plots of the normalised difference (**Single60_Dual40** - **Ctl**) of the wind forecast RMS error for 24- and 48-hour forecasts. The forecast impact is positive especially polewards of latitude 50° and for short range forecasts. From day 4-5 onwards the forecast impact is mainly neutral (not shown). Comparable results are obtained with the **Single50** experiment.

3.4 Discussion

Both single and dual Metop-A,B AMVs are very interesting for numerical weather prediction. The spatial coverage of the currently used AMVs in the ECMWF system is equatorward of $55\text{--}60^\circ$ latitude for GEO satellites and poleward of 70° latitude for the LEO satellites. Thus, in both hemispheres there is a $10\text{--}15^\circ$ gap in the AMV coverage. EUMETSAT processed Metop AMVs have excellent coverage over that area and using them in data assimilation would help to fully close the gap. In addition, enhancing the use of polar winds in general is desirable as MODIS AMVs from Terra have not been used actively since July 2013 due to degraded data quality and NOAA-16 has not been available after June 2014.

The quality of the Metop AMVs has significantly improved during the recent years. Currently for the single Metop-A,B AMVs the speed bias is within $\pm 0.5 \text{ ms}^{-1}$ at mid and low levels from where the majority of the observations originate. At high levels a negative speed bias up to -2 ms^{-1} is seen. The new dual Metop-A,B AMVs have quite similar characteristics to the single Metop-A,B AMVs at high latitudes. Over the tropics a

large positive wind speed bias is seen and the use of data is not considered. Overall, GEO AMVs are already giving excellent AMV coverage over that region.

Impact studies indicate benefits from using the Metop-A,B AMVs in the ECMWF system. Observation fit statistics show mainly neutral impact but verification against each experiment's own analysis indicate positive impact at high latitudes especially for 24 h to 96 h forecasts. For longer forecast ranges the impact is neutral. Comparable results are obtained when single Metop-A,B AMVs are used polewards from 60° N/S, and dual Metop AMVs are used between latitudes 40° and 60° or single Metop-A,B AMVs are used polewards from 50° N/S. In the latter case the gap between AMVs from GEO and LEO satellites is not completely closed. This configuration could serve as a backup plan in case dual Metop-A,B AMVs would not be available at some point. Operational usage of the EUMETSAT processed single and dual Metop-A,B AMVs was activated on 4th February 2016 in the ECMWF system.

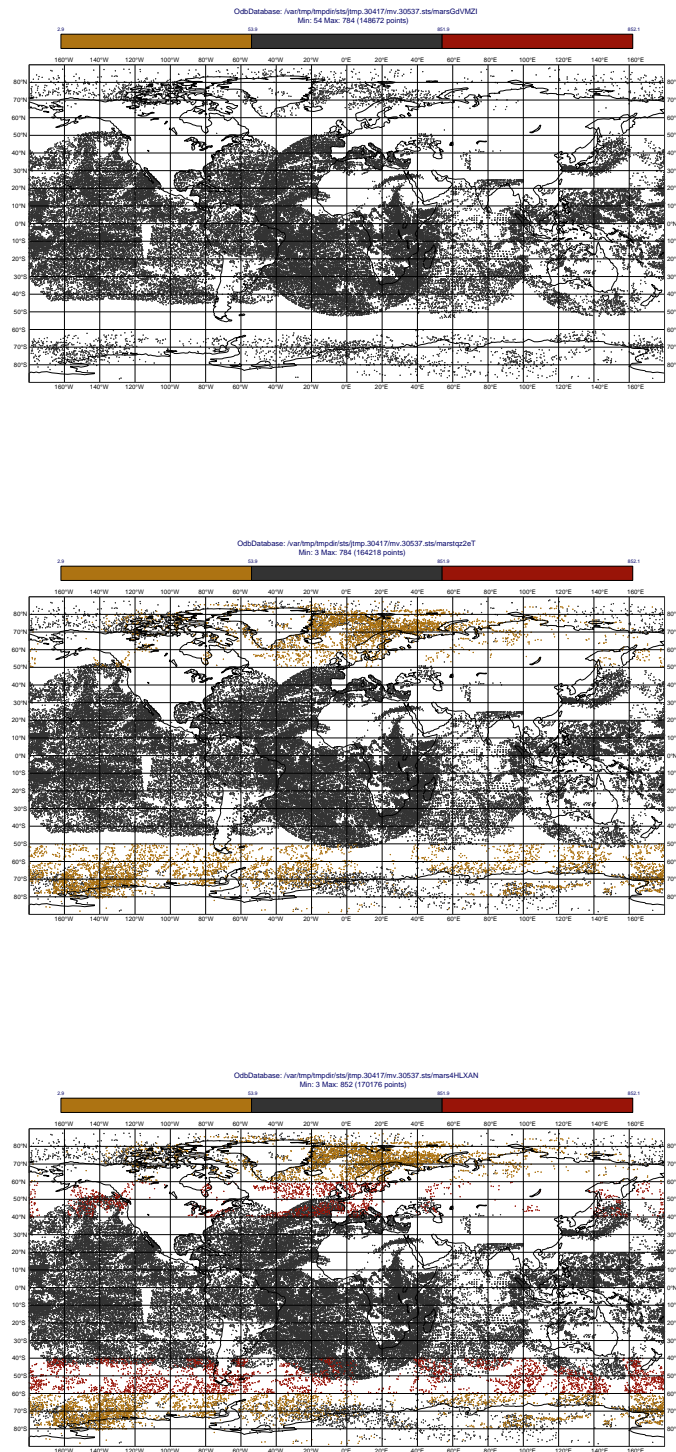


Figure 8: Sample coverage of active AMVs on 1st March 2015 12 UTC cycle. Upper panel is for **Ctl**, middle panel for **Single50** and lower panel for **Single60_Dual40** experiment, respectively. Active single Metop-A and Metop-B AMVs are marked with brown and dual Metop-A,B AMVs with dark red, all other AMVs are marked with grey.

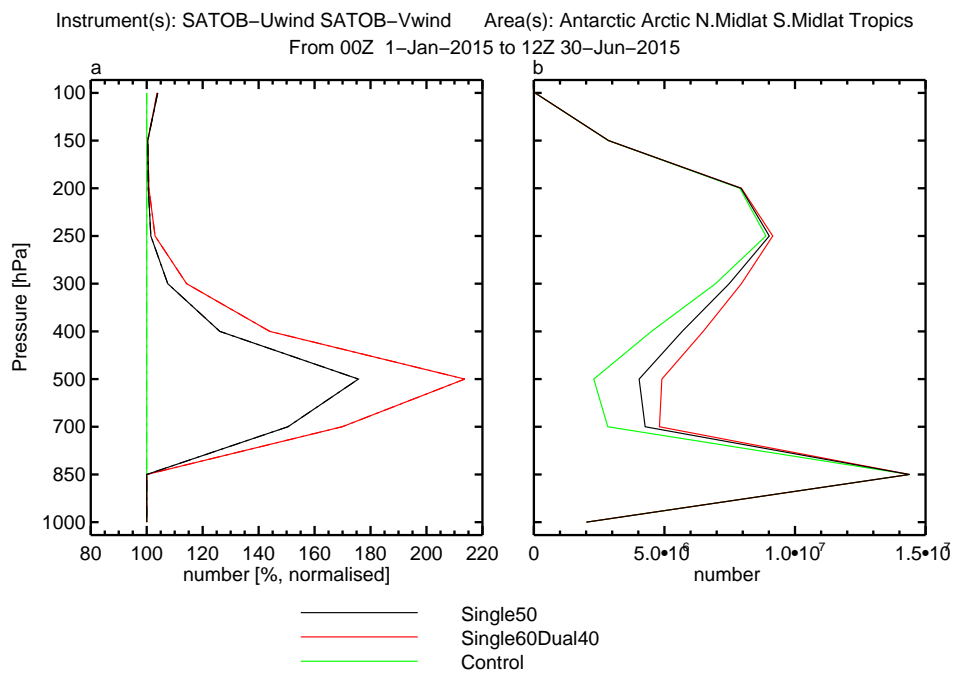


Figure 9: The number of active AMVs in the **Ctl** (green), **Single50** (black) and **Single60_Dual40** (red) experiments (right panel) and the relative increase in the used AMVs (left panel).

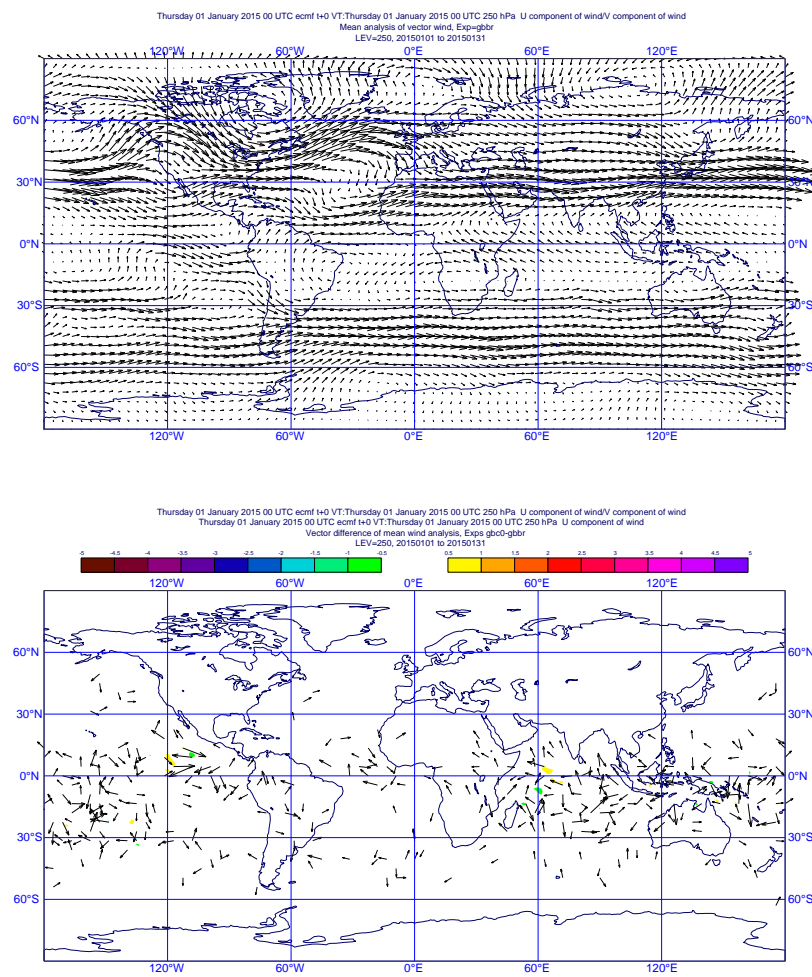


Figure 10: The mean wind analysis for the **Ctl** experiment at 250 hPa (upper panel) and the vector difference of the mean wind analysis between the **Ctl** and **Single60_Dual40** experiments (lower panel) for January 2015.

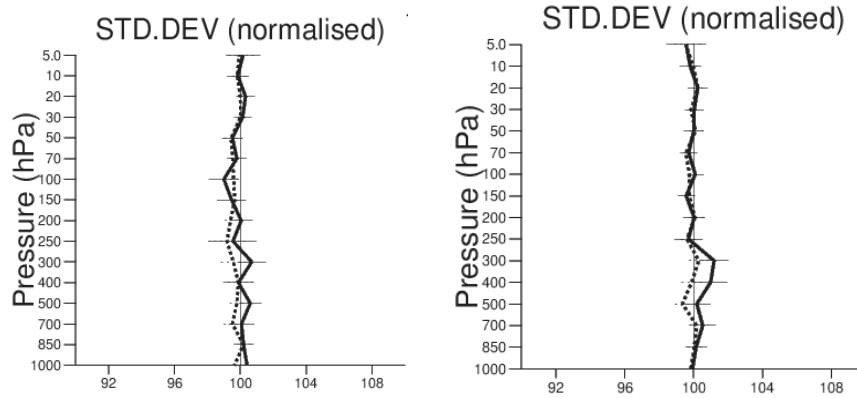


Figure 11: Normalised OmB standard deviation for radiosonde wind observations over the Southern polar cap (left panel u-component, right panel v-component).

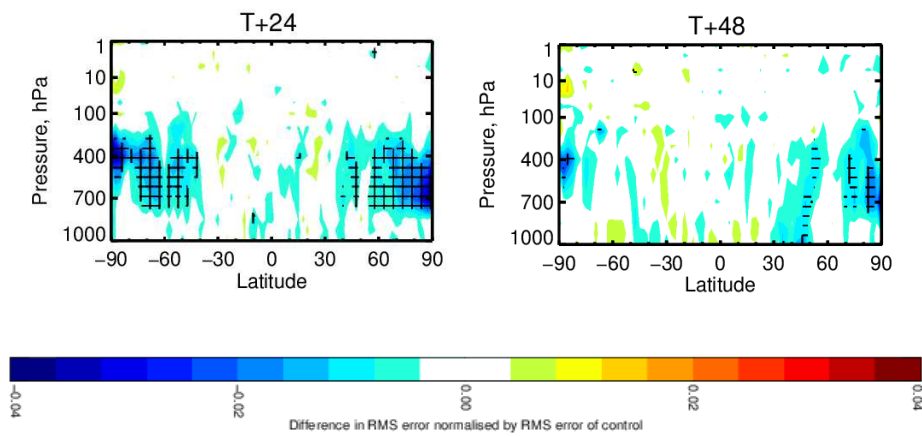


Figure 12: Zonal plots of the normalised difference (Single60_Dual40 - Ctl) wind forecast RMS error for 24- and 48-hour forecasts. Blue shades indicate positive impact and green and red shades negative impact. The considered period is 1.1-30.6.2015

4 Preparing for the arrival of GOES-R AMVs

A new AMV nested tracking algorithm has been developed for the Advanced Baseline Imager (ABI) to be flown on NOAA's future GOES-R satellite. The new algorithm captures the dominant motion in each target scene from a set of local motion vectors derived for each target scene. The dominant motion is taken to be the average of the local displacements of points belonging to the largest cluster. This approach prevents excessive averaging of motion that may be occurring at multiple levels or at different scales that can lead to a slow speed bias and poor quality AMVs. A representative height is assigned to the dominant motion vector through the use of cloud heights from pixels belonging to the largest cluster. The algorithm has been demonstrated to significantly improve the slow speed bias typically observed in AMVs derived from satellite imagery (Daniels et al., 2012).

In preparation for the use of GOES-R AMVs in NWP centres, NOAA/NESDIS has provided a proxy dataset that uses the nested tracking AMV algorithm. The proxy dataset covers 15.-30.6.2014 and is based on imagery from the Spinning Enhanced Visible and Infrared Imager (SEVIRI) onboard Meteosat-10. IR, cloudy WV, short wave IR (NIR), and VIS AMVs have been derived. The nested tracking algorithm provides several new parameters giving information about the characteristics of the cluster used in the AMV tracking as well as uncertainties in the height assignment process. The results obtained in the ECMWF system have been compared to those of the University of Wisconsin-Madison/Cooperative Institute for Meteorological Satellite Studies (CIMSS) in the framework of the GOES-R Visiting Scientist Program. The work has been done together with Sharon Nebuda from the University of Wisconsin-Madison.

The parameters that have been investigated and considered for quality control purposes in the NCEP GFS system at the University of Wisconsin-Madison/CIMSS include the following:

- Forecast independent quality indicator, QI
- Expected error, EE
- Expected error normalised by the AMV wind speed, NEE
- Standard deviation of displacements divided by the magnitude of the average displacement (1st vector), PCT1
- Pressure error in hPa estimated from cloud retrieval algorithm, PERR
- Cluster size in pixels (1st vector), MX1
- Number of clusters (1st vector), NOC1
- The range of cloud top pressure in the cluster, DCP
- Median optical depth, ODMD

Nebuda et al. (2014) have found the forecast independent QI, NEE and PCT1 to be most useful for the AMV quality control in the NCEP GFS system. The new parameter PCT1 is the standard deviation of the cluster's displacement of points divided by the distance the cluster moved. The cluster's motion vector is the average displacement of points divided by the time between scenes. For large values of PCT1, the cluster may be undergoing deformation and/or traveled a small distance which could decrease the accuracy of this data. In clusters with large values of PCT1, the AMVs show a slow speed bias with respect to radiosondes as well as when compared to the GFS background. Small values of PCT1 have been shown to be associated with AMVs which have positive speed departures (Nebuda et al., 2014).

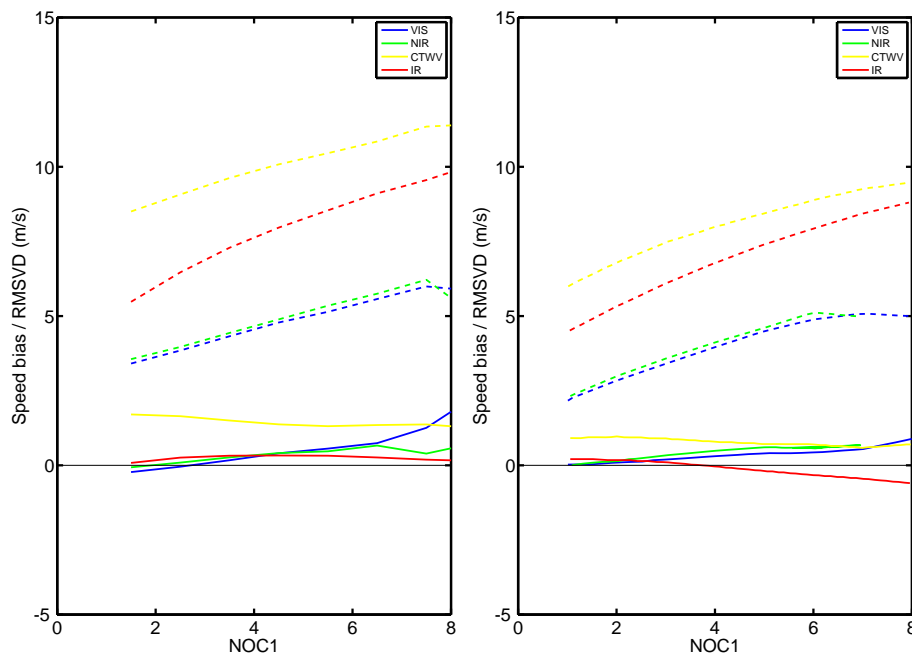


Figure 13: OmB wind speed bias (solid line) and RMSVD (dashed line) for different NOC1 values. Left panel shows statistics for the ECMWF system (15.-30.6.2014) and the right panel for the GFS system (November 2013). Blue is VIS, green short wave IR, yellow cloudy WV and red IR AMVs, respectively.

Investigations of the behaviour of the OmB statistics for the different parameters in the ECMWF system covering 15.-30.6.2014 show results that are generally in line with Sharon Nebuda's results with the NCEP GFS system for data covering November 2013. (NCEP GFS OmB statistics were not re-calculated for 15.-30.6.2014.)

Figure 13 shows the OmB wind speed bias (solid line) and RMSVD (dashed line) for different NOC1 values, left panel shows statistics for the ECMWF system and the right panel for the GFS system. In both systems the RMSVD increases for increasing NOC1 values while the OmB speed bias is less dependent on NOC1. Figure 14 shows a scatter plot of observed wind speed versus ECMWF first guess wind speed for the IR AMVs. In the left panel all data is shown and in the right panel a criterion $\text{NOC1} \leq 6$ is used. Using this criterion for NOC1 removes some outliers from the data, the total data count decreases by about 8%.

Figure 15 shows the same than Fig. 13 but for the parameter PCT1. Again the two systems show similar behaviour, large bias and RMSVD for small values of PCT1. Figure 16 is similar to Fig. 14 but now in the right panel criterion $0.04 \leq \text{PCT1} \leq 0.5$ from Nebuda et al. (2014) is used. Again using the criterion removes outliers and the total data count decreases by about 17%. However, at the same time the majority of the high wind speed observations are filtered out which is not necessarily desirable.

The general conclusion from the investigations in the ECMWF system is that the traditional forecast independent QI remains the effective parameter to be used to remove low quality observations. In terms of removing outliers and not changing the wind speed distribution, the most potential for quality control purposes are seen with the new parameters PERR, MX1, NOC1, DCP and ODMD in addition to the traditional QI in the ECMWF system. As an example, Fig. 17 shows the number of observations (upper panel), OmB wind speed bias (middle panel) and RMSVD (lower panel) for all IR observations (left) and after using the following quality criteria:

- Forecast independent QI ≥ 70

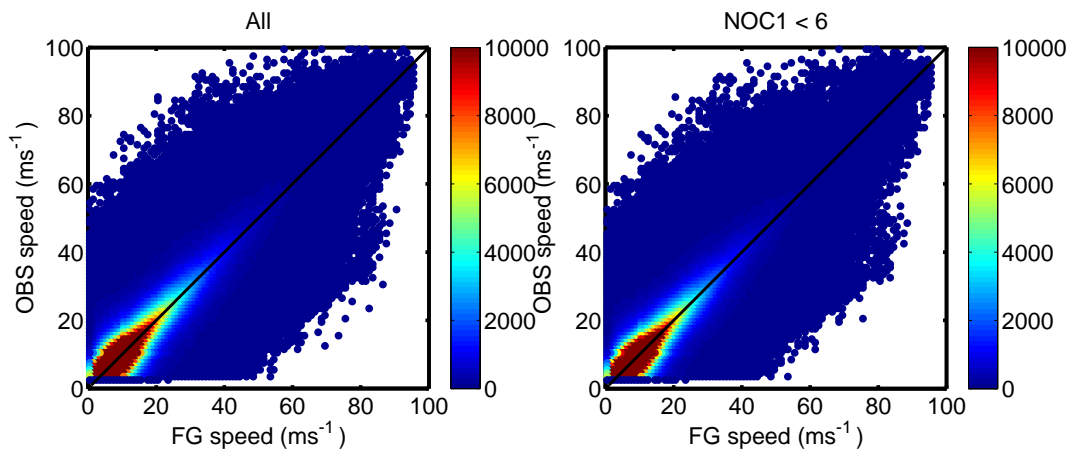


Figure 14: Scatter plot of observed wind speed versus ECMWF first guess wind speed for IR AMVs. Left panel shows all data and the right panel data with criterion $NOC1 \leq 6$. The covered period is 15.-30.6.2014.

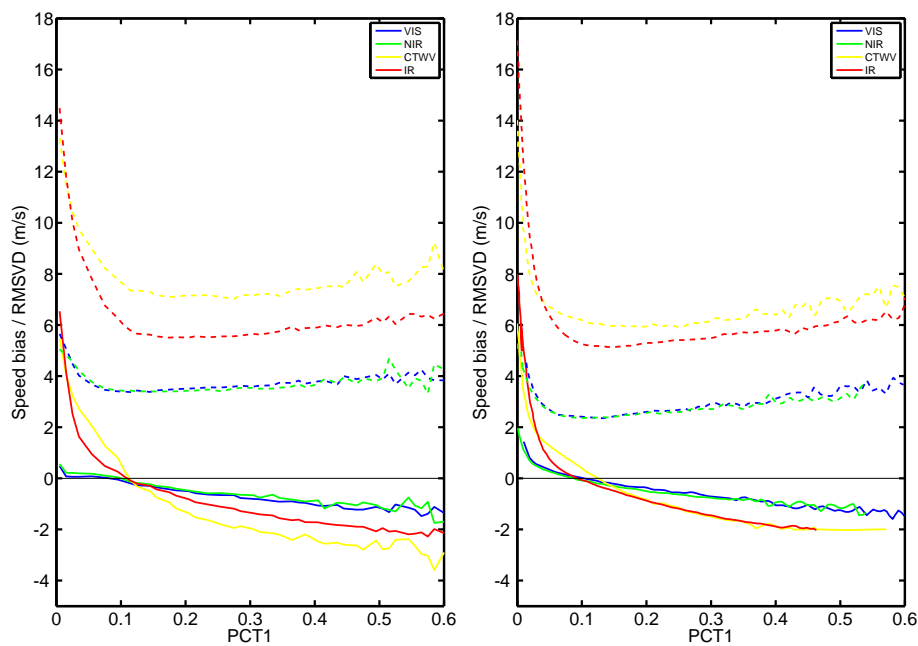


Figure 15: Same as Fig. 13 but for PCT1.

- $PERR \leq 150$ hPa
- $MX1 \geq 25$
- $NOC1 \leq 6$
- $ODMD \geq 0.5$
- $50 \leq DCP \leq 600$

The tested quality criteria are based on plots similar to Fig. 13 and the used limits are relatively relaxed. Using

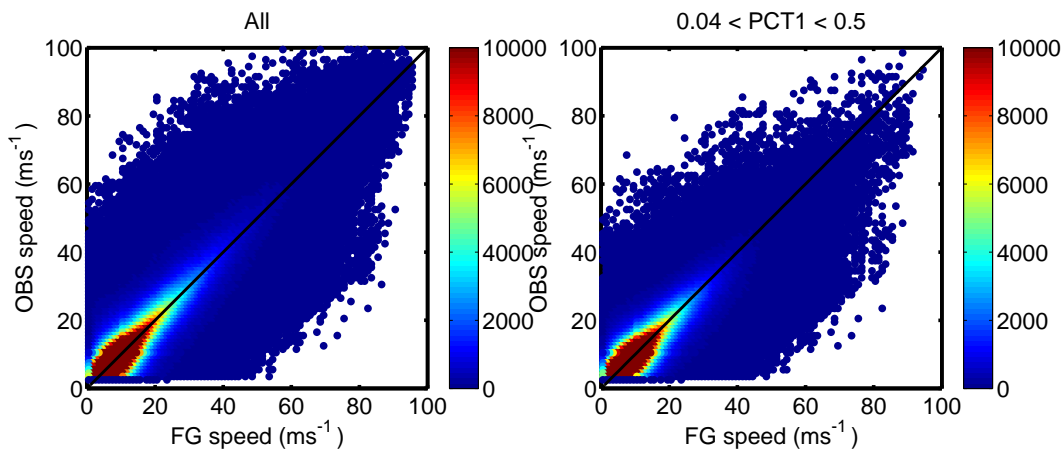


Figure 16: Same as Fig. 14 but for PCT1.

the quality criteria removes 35% of the observations and bias and RMSVD statistics are somewhat improved. Figure 18 shows the same as Fig. 17 but for observations accepted by the first guess check (left) and when the quality criteria are applied for the accepted AMVs (right). Using the quality criteria on top of the first guess check rejects 30% more observations but the OmB bias and RMSVD statistics are not further improved with the chosen limits. However, the additional quality criteria might allow a relaxation of the first guess check, which would be desirable. Data assimilation experiments and testing different variations for the quality criteria would be required to investigate whether using the new parameters for quality control would have positive impact on analysis and forecasts. For this kind of investigations a longer data set would be required.

One of the most interesting new parameters is PERR, which is an estimate of the pressure error provided by the cloud retrieval algorithm. PERR shows some potential to be used in quality control. However, it would affect different cloud types in different ways. The new nested tracking algorithm provides information also about the cloud type which is dominant in the tracking scene. Figure 19 shows the PERR for different cloud scenes for cloudy WV AMVs. If it is assumed that the biggest cluster used to make the AMV is the same type as the dominant type in the scene, this distribution indicates the clusters of opaque ice have the smallest uncertainty in their cloud top pressure. If a quality control threshold would be chosen for PERR, in case of WV AMVs it would impact the cirrus scenes most. For VIS, IR and short wave IR AMVs majority of the observations are from water scenes.

PERR could be a very interesting parameter especially for the observation error specification. The ECMWF system uses situation dependent observation errors for AMVs (Salonen and Bormann, 2013). Currently the height errors are estimated based on long term model best-fit pressure statistics. Another option would be to use producer provided estimates but they are not yet operationally available. Figure 20 shows the mean PERR (blue line) and the standard deviation of assigned pressure minus the model best-fit pressure (black line) at different levels for IR AMVs. In general, the height error estimates from the cloud retrieval algorithm are smaller in magnitude than the best-fit pressure based estimates for the studied period. Thus, using PERR for the situation dependent observation errors instead of the best-fit pressure statistics would result in smaller observation errors. Data assimilation experiments would be required to investigate the forecast impact.

We have investigated the effect of using PERR for observation error specification, instead of a constant value. For technical reason, we estimate the wind error due to height assignment as $abs(\Delta p \times shear)$, where Δp is PERR or a constant value of 80 hPa and $shear$ is the difference in wind speed 50 hPa above and below the assigned AMV height. Figure 21 shows the wind speed OmB standard deviation as a function of $abs(\Delta p \times$

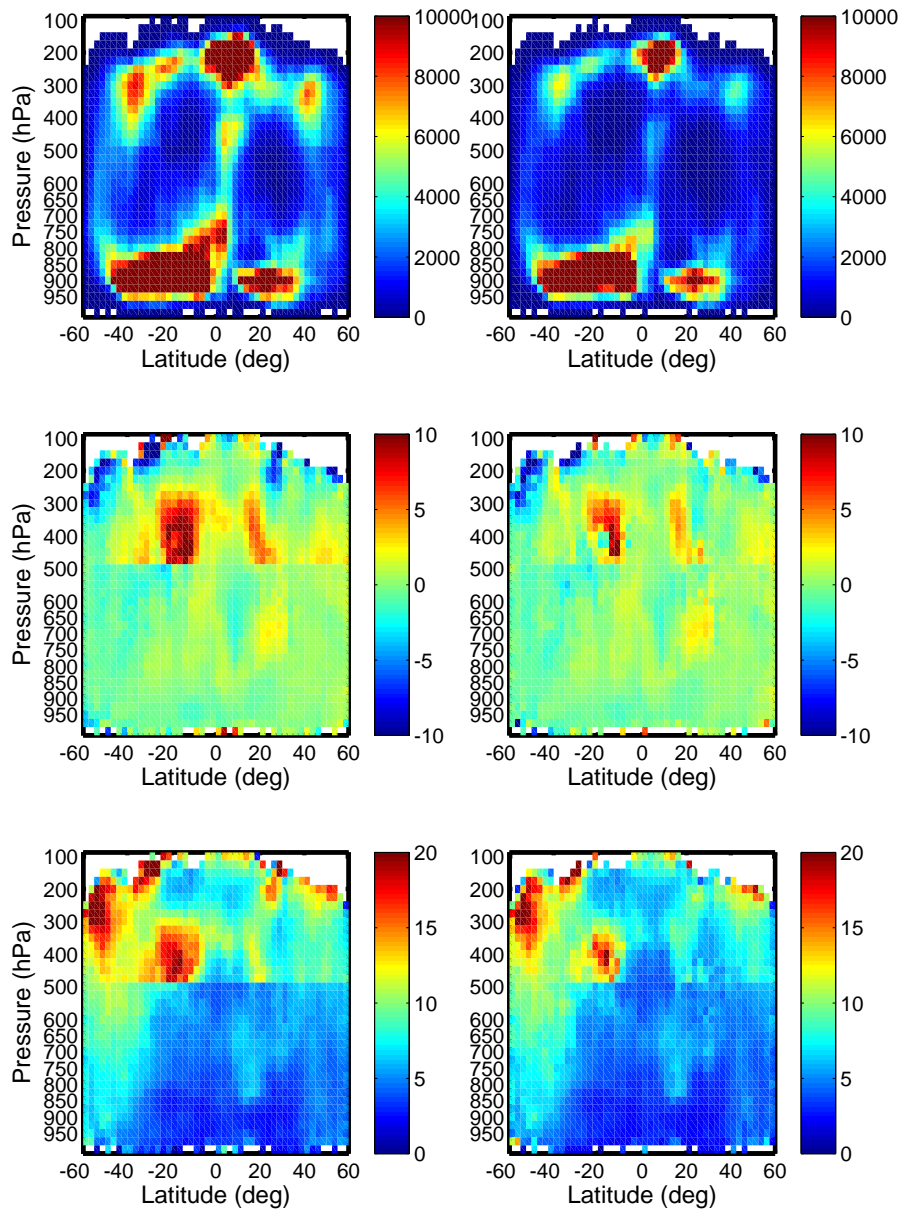


Figure 17: Zonal plots of the number of observations (upper panel), OmB wind speed bias (middle panel) and RMSVD (lower panel) for all IR observations (left) and after using the quality criteria.

shear). In general, the OmB standard deviation increases with $abs(\Delta p \times shear)$ indicating that the increase in the OmB standard deviation is related to AMVs with increased error in wind due to error in the height assignment. The PERR and constant value of 80 hPa show quite similar behaviour. It would be very interesting to further investigate the use of PERR in defining the situation dependent observation errors. Also potential of some other of the new parameters provided with the nested tracking algorithm could be investigated to further refine the AMV observation errors.

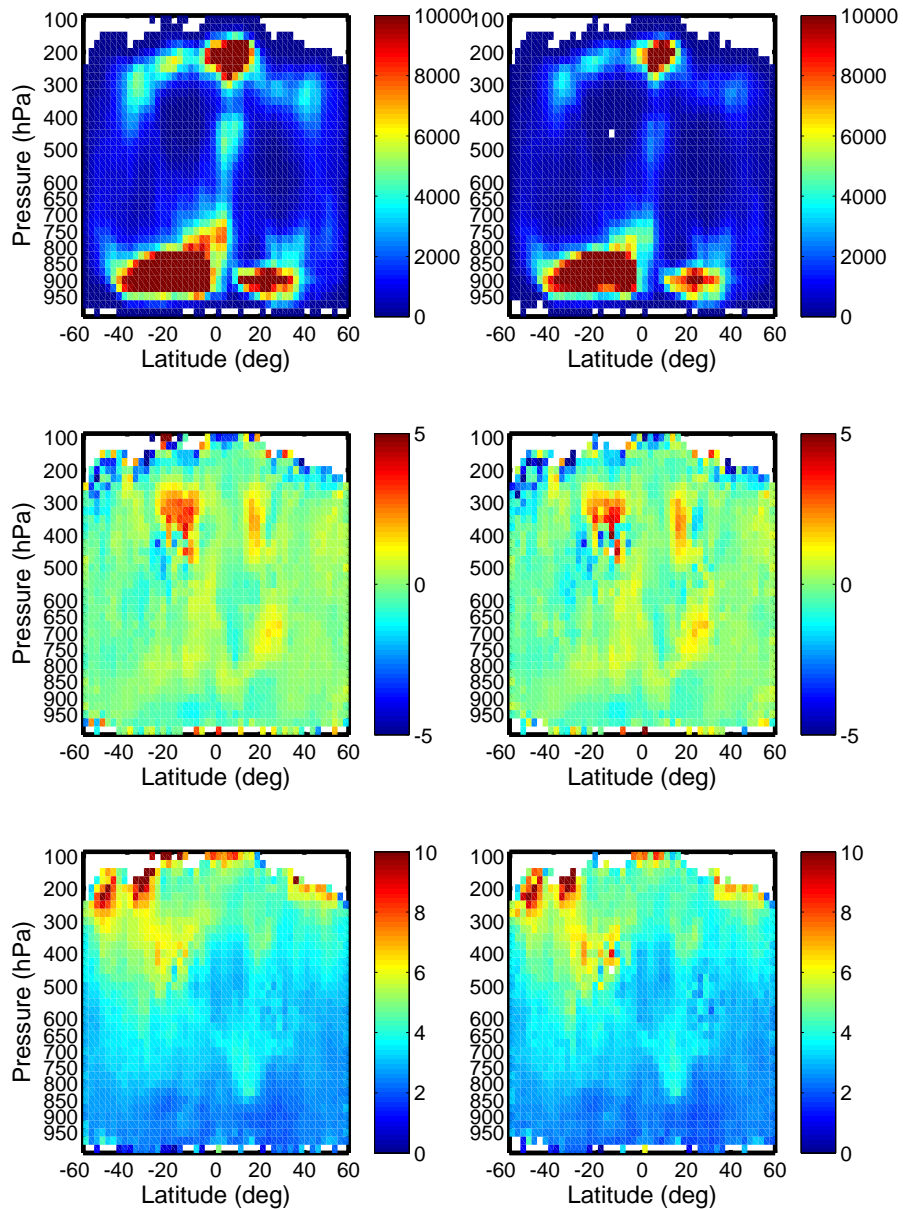


Figure 18: Same as Fig. 17 but for observations accepted by the first guess check (left) and when the quality criteria are applied for the accepted AMVs. (Note different scale for OmB bias and RMSVD as in Fig. 17.)

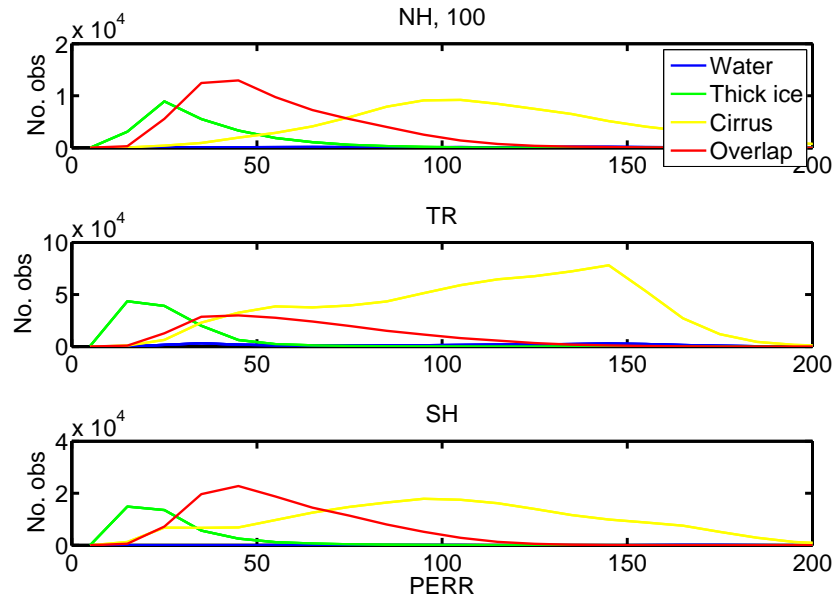


Figure 19: PERR for different cloud scenes for cloudy WV AMVs. Blue is water clouds, green thick ice, yellow cirrus and red overlapping clouds

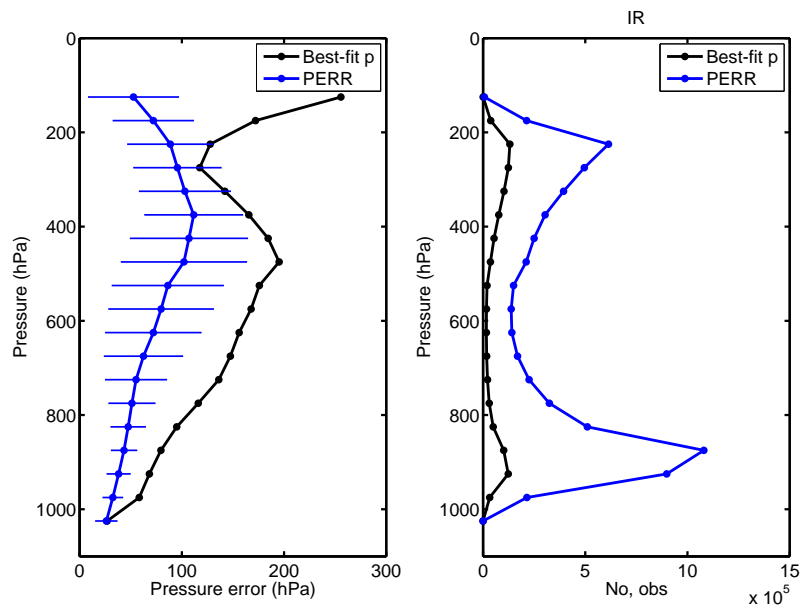


Figure 20: Mean PERR (blue line) and the standard deviation of assigned pressure minus the model best-fit pressure (black line) at different levels for IR AMVs (left panel). Number of observations (right panel).

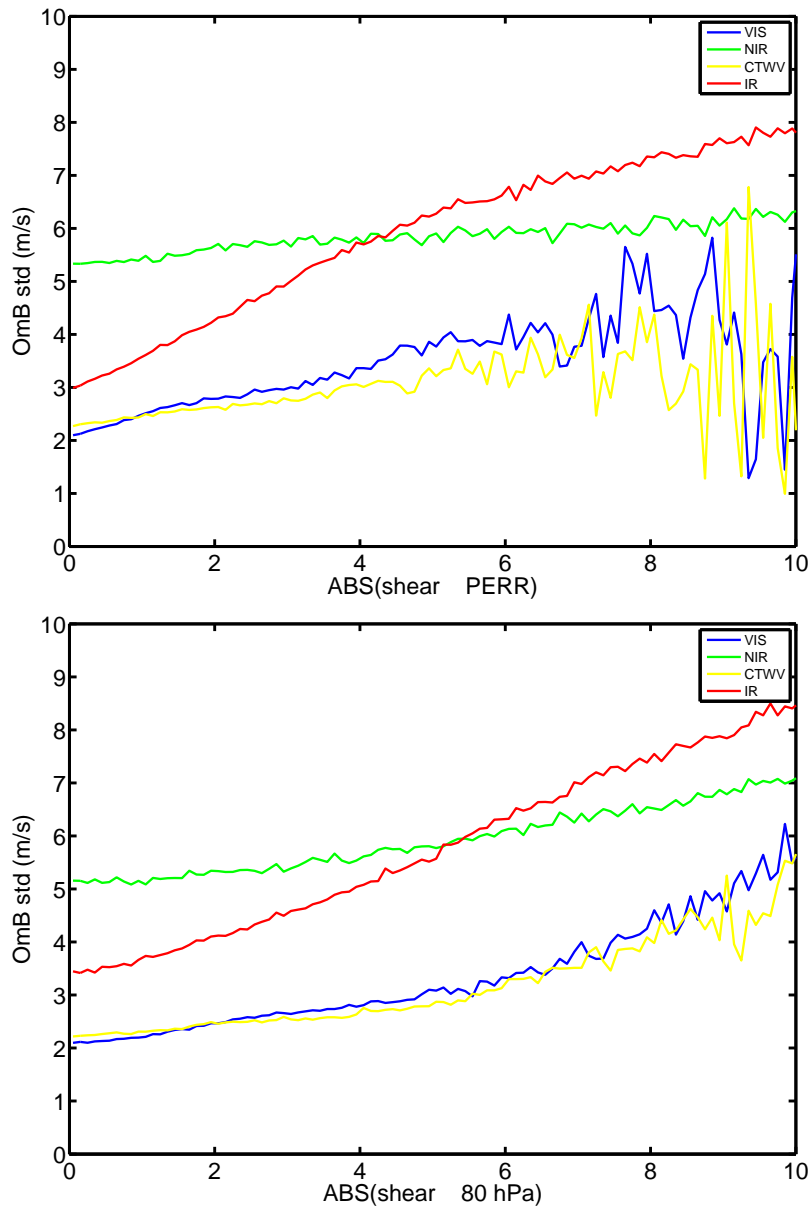


Figure 21: The wind speed OmB standard deviation as a function of $abs(\Delta p \times shear)$. Blue is VIS, green short wave IR, yellow cloudy WV and red IR AMVs, respectively.

5 Investigations on accounting for the systematic height assignment errors for AMVs in NWP

AMVs are typically interpreted as single level wind observations assigned to a representative height which is cloud top for high and mid level clouds and cloud base for low level clouds. Comparison to radiosonde (Velden and Bedka, 2009) and lidar observations (Folger and Weissmann, 2014; Weissmann et al., 2013) as well as results from simulation framework (Hernandez-Carrascal and Bormann, 2014) suggest benefits from interpreting AMVs as layer averages or as single level wind but within the cloud. Height assignment is considered to be one of the most significant error sources for AMVs.

Taking into account the AMV height assignment uncertainties through situation dependent observation errors has been very beneficial in the ECMWF system (Salonen and Bormann, 2013). An interesting question is: Could we further improve the use of AMVs by taking into account systematic height assignment errors? Initial investigations in the ECMWF system have shown promising results from using the traditional single-level observation operator together with the height re-assignment based on long-term model best-fit pressure statistics (Salonen and Bormann, 2015). Experimenting with layer averaging observation operator has shown more mixed results and is not further considered here.

In this section the focus is on estimating the systematic height errors with two independent methods, model best-fit pressure and lidar height correction. The work has been done in co-operation with Kathrin Folger and Martin Weissmann from the Hans-Ertel-Centre for Weather Research. The aim is to compare the systematic height error estimates in order to investigate and explain the similarities and differences. In the end some preliminary results from an impact study are discussed.

5.1 Estimating systematic height errors

Model best-fit pressure

The model best-fit pressure is defined as the pressure level where the observed wind and the model wind agree the best. Comparison of the best-fit pressure statistics for the Met Office and the ECMWF data assimilation systems has shown that the statistics are generally very similar to each other, suggesting that the pressure differences are not strongly dependent on the data assimilation system (Salonen et al., 2015).

The main advantage of the best-fit pressure is that it can be defined for every AMV observation. Thus, height assignment error characteristics can be easily investigated for each satellite, channel and height assignment method, at all locations where AMVs are available. However, it is important to note that the best-fit pressure also includes contributions from errors in the model background and it is not always possible to define an unambiguous value for it.

When analysing the best-fit pressure statistics, it is necessary to ensure that the best-fit pressure provides a meaningful estimate for the pressure level of the observed AMV. A secondary or a very broad minimum can lead to best-fit pressures that are not very meaningful. Similarly, at times there is no good agreement between the AMV and the model wind at any pressure level, either due to tracking errors or large forecast errors. These kind of cases are filtered out from the statistics.

It is worth to emphasize that the systematic height error estimates must be based on long-term best-fit pressure statistics, typically at least one month worth of data.

Lidar correction

The CloudAerosol Lidar and Infrared Pathfinder Satellite Observations (CALIPSO) based lidar height correction method is described in [Folger and Weissmann \(2014\)](#). AMV winds are compared with radiosonde winds that are vertically averaged over layers of varying depth relative to the originally assigned AMV height and for layers relative to the CALIPSO lidar cloud-top height. On average, the best fit between AMVs and radiosonde winds is obtained for a 120 hPa deep layer below the lidar cloud top. The level of best fit is the mean pressure of that layer, i.e. a discrete level 60 hPa below the lidar cloud top.

There are some requirements that have to be fulfilled that an AMV is considered for the lidar height correction. The main point is that AMV and CALIPSO lidar observation have to be within a distance of 50 km and a time difference of 30 min. In addition, an outlier removal is performed. Only AMVs which are at maximum 100 hPa above and 200 hPa below the nearby lidar cloud top are taken into account. This interval is chosen to account for the fact that the lidar observation and the AMV may see different clouds because of the temporal and/or horizontal displacement and is based on the assumption that AMVs represent the wind below the actual cloud top.

Direct AMV height correction can only be applied to AMVs for which the collocated CALIPSO observations are available. However, a more general approach is possible when a mean adjustment calculated from a large sample of AMV/lidar collocations is considered ([Folger and Weissmann, 2015](#)). Here, the mean adjustment is compared to the best-fit pressure based approach.

5.2 Comparison of the methods

Systematic height assignment error estimates obtained with the two independent methods have been compared for geostationary satellites Meteosat-7, Meteosat-10, MTSAT-2, GOES-13 and GOES-15. The considered period is 1.4-13.6.2013. CALIPSO lidar observations are not available for 10.4-15.4 and 16.5-27.5 and these days have been excluded from the comparison. Only AMVs with a forecast independent QI greater than 80 have been considered. The systematic height assignment error estimates are investigated separately for IR, VIS and WV channels but there is no additional separation based on height assignment method.

In the following, positive (negative) values indicate that the assigned AMV pressure is on average higher (lower) than the best-fit pressure/the lidar level of best fit. In terms of height that means that the observation is lower (higher) in the atmosphere than the best-fit pressure/the lidar level of best fit.

Figure 22 shows the best-fit pressure based systematic height error estimates (left panel) and the lidar correction based systematic height error estimates (right panel) for GOES-15 IR AMVs. The grey bars indicate the number of observations. The shapes of the curves are similar for both methods. This is generally the case for IR AMVs also from other satellites. At low levels typically the magnitudes of the systematic height error estimates are the same. At midlevels and high levels some differences in the magnitude are seen. Typically if there is a difference in magnitude, the lidar based estimate is more negative than the best-fit pressure based estimate.

For WV AMVs generally at the heights from which most of the AMVs originate similarities between the methods are seen. However, again there are some differences in the magnitude. Figure 23 shows the same as Fig. 22 but for Meteosat-10 WV AMVs at midlatitudes as an example of the results. A similar shape is seen in the curves but there is a 25-50 hPa shift between the methods. The lidar based values are more negative (or less positive) than the best-fit pressure based values.

One possible explanation for the shift between the methods is that for the lidar correction the level of best fit is considered to be 60 hPa below the lidar cloud top at all heights. [Folger and Weissmann \(2014\)](#) show that a 100

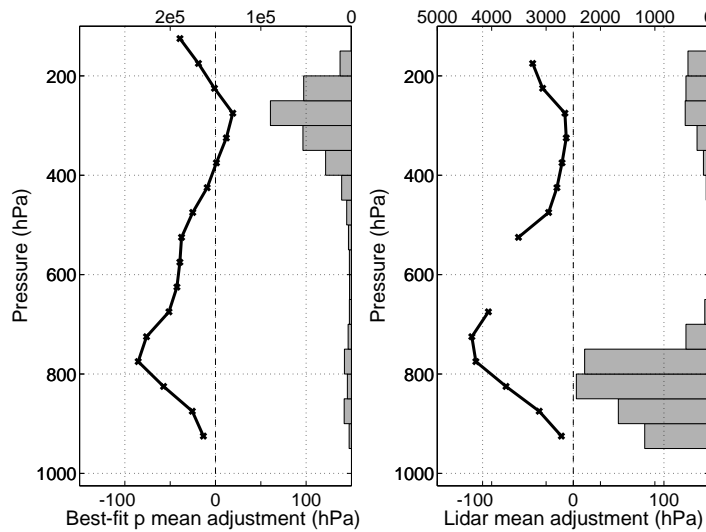


Figure 22: The best-fit pressure based systematic height error estimates (left panel) and the lidar correction based systematic height error estimates (right panel) for GOES-15 IR AMVs. The grey bars indicate the number of observations.

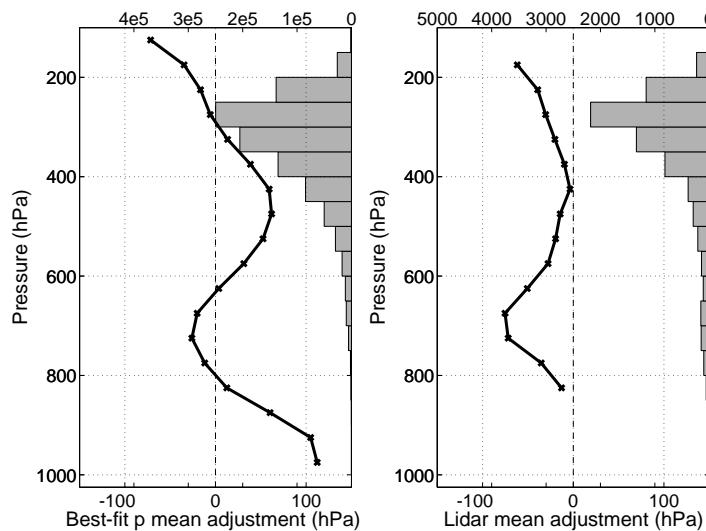


Figure 23: Same as Fig. 22 but for Meteosat-10 WV AMVs over midlatitudes.

hPa deep layer below the lidar cloud top also achieves very good results. In practise this means that the results for a level at 50 hPa below the lidar cloud top is basically almost equivalent to the 60 hPa considered in this comparison. This would result in lidar corrections of the same shape but shifted 10 hPa to the right. If the level of best fit varies slightly at different heights, the shift seen between the methods might decrease.

Figure 24 shows the same as Fig. 22 but for Meteosat-7 VIS AMVs at midlatitudes. In this particular case the best-fit pressure and lidar based systematic height error estimates are almost the same. Overall, for VIS AMVs a similar shape for both methods is seen both in the midlatitudes and tropics. If there is a difference in the magnitude, it is opposite to what is seen for IR and WV AMVs, i.e. the best-fit pressure bias is indicating more negative bias than the lidar correction.

Overall, it can be concluded that the two independent methods to estimate systematic height errors for AMVs

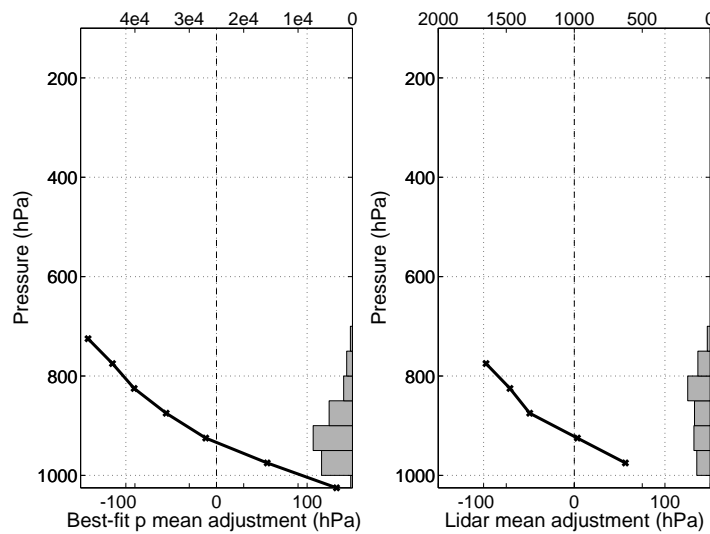


Figure 24: Same as Fig. 22 but for Meteosat-7 VIS AMVs over the midlatitudes.

support each other. Generally the shapes of the curves are similar. For IR and VIS AMVs the magnitudes are also comparable especially at low levels. For WV winds and for high level IR winds some differences are seen in the magnitude. Shifts of 20-60 hPa are seen between the methods and typically the lidar correction is indicating more negative values than the best-fit pressure statistics.

5.3 Results from preliminary impact assessment

The information on systematic height assignment errors can be used to re-assign the AMVs to a more representative level. As a first trial the re-assignment has been done based on the best-fit pressure statistics discussed in the previous subsection. In practice each AMV height is re-assigned based on the bias statistics before calculating the model counterpart for the observation.

The height re-assignment has been tested over a winter season (1.12.2014-28.2.2015) and a summer season (1.5-31.7.2015) with the ECMWF IFS cycle 41r1 at T639 resolution, 137 vertical levels, and 12-hour 4D-Var. All operationally assimilated conventional and satellite observations were used in the experiments. In the following two experiments are considered:

- **Ctl**: Single-level observation operator with AMVs at originally assigned height
- **Re-assigned**: Single-level observation operator with AMV height re-assignment based on the best-fit pressure statistics

OmB statistics can be used to investigate if the fit of the observations to the model background has improved as a result of the introduced changes. Figure 25 shows the OmB wind speed bias (left panel) and RMSVD (right panel) for GOES-13 AMVs. The solid line indicates the **Ctl** experiment and dashed line the **Re-assigned** experiment. Only AMVs that are actively used in the analysis are considered. In general the OmB wind speed bias and RMSVD are somewhat increased for the **Re-assigned** experiment compared to the **Ctl** experiment, especially below 550 hPa. Thus, re-assigning the AMV heights has slightly degraded the fit between the AMVs and background which is unexpected. Similar results are seen also for GOES-15, Meteosat-7 and Meteosat-10. The only exception is MTSAT-2 which shows also some improvements in the OmB statistics (Fig. 26).

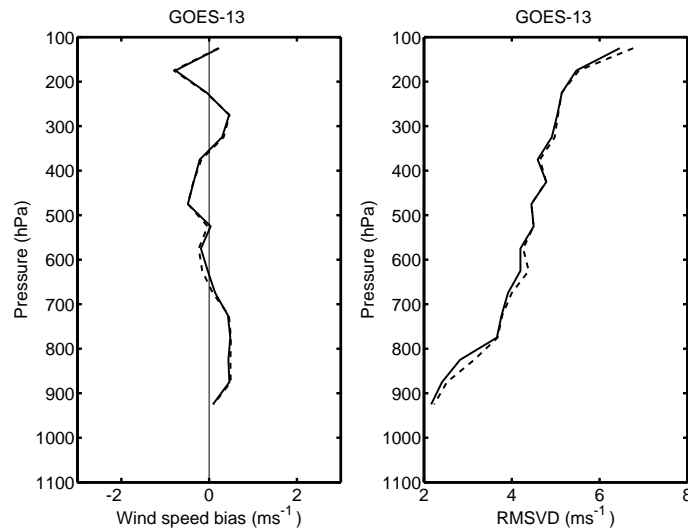


Figure 25: OmB wind speed bias (left panel) and RMSVD (right panel) for GOES-13 AMVs. The solid line indicates the **Ctl** experiment and dashed line the **Re-assigned** experiment. Only AMVs that are actively used in the analysis are considered.

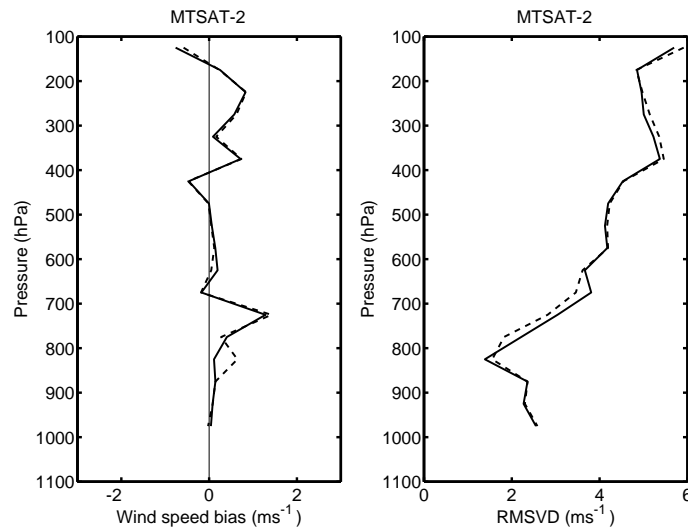


Figure 26: Same as Fig. 25 but for MTSAT-2 AMVs.

The reasons for the worse OmB statistics are not fully understood. One possible explanation is changes in the characteristics of the height assignment biases. Figure 27 shows the best-fit pressure based systematic height error estimates for Meteosat-10 WV AMVs from the best-fit pressure - lidar comparison period 1.4-13.6.2013 (left panel, same as Fig. 23 left panel) and from the **Ctl** experiment (right panel, winter period 1.12.2014-28.2.2015 only). Comparison of the best-fit pressure statistics from the two periods indicate that the systematic height error estimates have not significantly changed. This is the case for other satellites as well except GOES-13 and GOES-15 low level IR and VIS AMVs where the systematic height error estimates have decreased about 50 hPa in magnitude at 850 - 700 hPa levels. NOAA/NESDIS introduced algorithm improvements related to low level winds to the GOES AMV product in May 2014 which explains the change in the magnitude of the systematic height error estimates. In the **Re-assigned** experiment the estimates from the lidar comparison

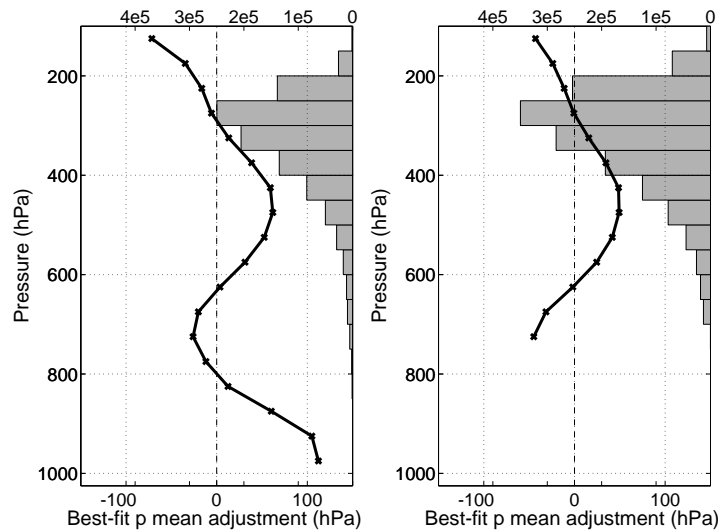


Figure 27: The best-fit pressure based systematic height error estimates 1.4-13.6.2013 (left panel) and 1.12.2014-28.2.2015 (right panel) for Meteosat-10 WV AMVs over the midlatitudes.

period are used. Thus, the experiment set up is not completely optimal. The systematic height error estimates should always be updated after data providers introduce changes into their AMV processing. However, this does not appear to provide a complete explanation for the poorer OmB statistics, and further investigations are required to understand this.

Figure 28 shows the normalised change in OmB standard deviation for other wind observations (radiosonde, pilot and wind profiler observations). The reference is the **Ctl** experiment. Thus, values below 100% indicate improvements in the observation fit statistics while values above 100% indicate degradation. The horizontal bars indicate 90% confidence range. The OmB fit for these wind observations has slightly improved in the **Re-assigned** experiment but the changes are not statistically significant.

It can be concluded that the observation fit statistics give somewhat mixed results. Generally the fit of AMVs to the model background has slightly degraded while the fit of other wind observations has slightly improved as a consequence of re-assigning the AMV heights based on the model best-fit pressure based systematic height error estimates. For GOES-13 and GOES-15 low level IR and VIS AMVs the systematic height error estimates have not been up to date which most likely has some impact on the results.

To investigate the impact of taking into account the systematic height errors on longer range forecasts, verification against each experiment's own analysis has been done. Figure 29 shows the zonal plots of the normalised difference of the wind forecast RMS error for 2 to 5 day forecasts. The forecast scores indicate neutral to slightly positive impact. This result is encouraging and motivates further investigations.

5.4 Conclusions

The systematic height assignment errors for AMVs have been estimated with two independent methods, model best-fit pressure and lidar height correction. The comparison shows that the two methods generally support each other. For IR and VIS AMVs the magnitudes of the systematic height error estimates are comparable especially at low levels. For WV winds and for high level IR winds some differences are seen in the magnitude. Shifts of 20-60 hPa are seen between the methods and typically the lidar correction is indicating more pronounced

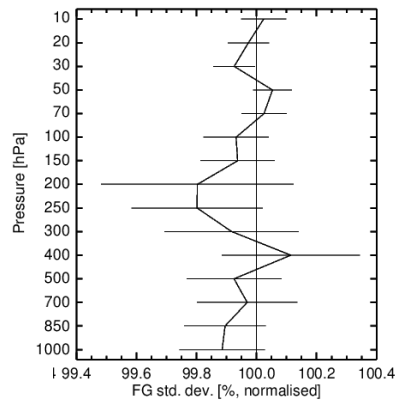


Figure 28: Normalised change in observation minus background (OmB) standard deviation for radiosonde, pilot and wind profiler observations. The winter (1.12.2014-28.2.2015) and a summer season (1.5-31.7.2015) are considered together.

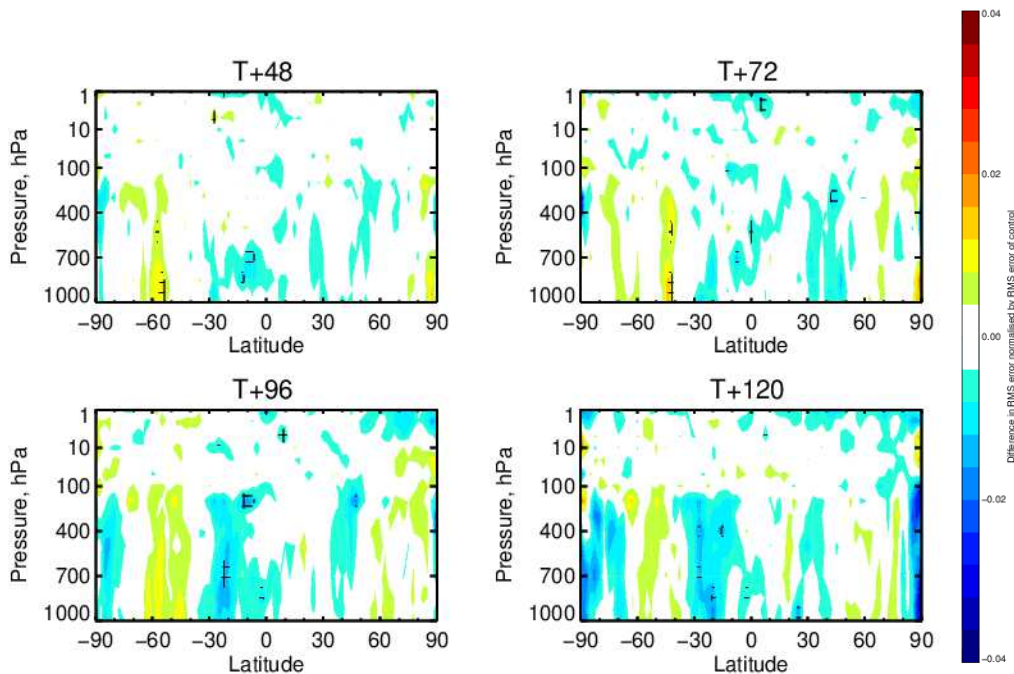


Figure 29: Zonal plots of the normalised difference (**Re-assigned - Ctl**) wind forecast RMS error for different forecast lengths. Blue shades indicate positive impact and green and red shades negative impact. The winter (1.12.2014-28.2.2015) and a summer season (1.5-31.7.2015) are considered together.

negative values, i.e. AMVs assigned too high in the atmosphere, than the best-fit pressure statistics.

Preliminary data assimilation experiments have been performed with the ECMWF system. The AMV heights are re-assigned based on the best-fit pressure statistics from the lidar comparison period. The observation fit statistics give somewhat mixed results. Generally the fit of AMVs to the model background has slightly degraded while the fit of other wind observations has slightly improved as a consequence of re-assigning the AMV heights. The forecast scores indicate neutral to slightly positive impact. The results are encouraging but further investigations are required.

Acknowledgements

Kirsti Salonen is funded by the EUMETSAT fellowship programme.

References

- Borde, R., Hautecoeur, O., Carranza, M., Doutriaux-Boucher, M., 2013. Recent changes and developments in EUMETSAT operational winds. Proceedings of the 2013 EUMETSAT Meteorological Satellite Conference, Vienna, Austria, 16-20 September 2013.
- Borde, R., Oyama, R., 2008. A direct link between feature tracking and height assignment of operational atmospheric motion vectors. Proceedings of the 9th International Wind Workshop, Annapolis, Maryland, USA, 14-18 April 2008.
- Daniels, J., Bresky, W., Wanzong, S., Bailey, A., Velden, C., 2012. Atmospheric motion vectors derived via a new nested tracking algorithm developed for the GOES-R advanced baseline imager (ABI). Proceedings of the 11th International Wind Workshop, Auckland, New Zealand, 20-24 February 2012.
- Folger, K., Weissmann, M., 2014. Height correction of atmospheric motion vectors using satellite lidar observations from CALIPSO. JAMC 53, 18091819.
- Folger, K., Weissmann, M., 2015. Lidar-based height correction for the assimilation of atmospheric motion vectors. JAMC Submitted.
- Forsythe, M., Saunders, R., 2008. AMV errors: a new approach in NWP. Proceedings of the 9th International Wind Workshop, Annapolis, Maryland, USA, 14-18 April 2008 EUMETSAT P.51.
- Hautecoeur, O., Borde, R., Doutriaux-Boucher, M., Carranza, M., 2014. EUMETSAT operational dual-metop wind product. Proceedings of the 12th International Wind Workshop, Copenhagen, Denmark, 16-20 June 2014.
- Hernandez-Carrascal, A., Bormann, N., 2014. Atmospheric motion vectors from model simulations. Part II: Interpretation as spatial and vertical averages of wind and role of clouds. J. Appl. Meteor. Climatol. 53, 65–82.
- Hoover, B., Santek, D., Lazzara, M., Dworak, R., Key, J., Velden, C., Bearson, N., 2012. High latitude satellite-derived winds from combined geostationary and polar orbiting satellite data. Proceedings of the 11th International Wind Workshop, Auckland, New Zealand, 20-24 February 2012.
- Lazzarra, M., Dworak, R., Santek, D., Hoover, B., Velden, C., Key, J., 2014. High-latitude atmospheric motion vectors from composite satellite data. JAMC 53, 534–547.

- Nebuda, S., Jung, J., Santek, D., Daniels, J., Bretsky, W., 2014. Assimilation of GOES-R atmospheric motion vectors (AMVs) in the NCEP global forecast system. Proceedings of the 12th International Wind Workshop, Copenhagen, Denmark, 16-20 June 2014.
- Qi, H., Daniels, J., Pennoeyer, W., Bailey, A., Augenbaum, J., 2014. Operational wind products at NOAA/NESDIS. Proceedings of the 12th International Wind Workshop, Copenhagen, Denmark, 16-20 June 2014.
- Salonen, K., Bormann, N., 2013. Winds of change in the use of Atmospheric Motion Vectors in the ECMWF system. ECMWF Newsletter 136, 23–27.
- Salonen, K., Bormann, N., 2015. Atmospheric Motion Vector observations in the ECMWF system: Fourth year report. EUMETSAT/ECMWF Fellowship Programme Research Report No.36.
- Salonen, K., Cotton, J., Bormann, N., Forsythe, M., 2015. Characterising AMV height assignment error by comparing best-fit pressure statistics from the Met Office and ECMWF data assimilation systems. JAMC 54, 225–242.
- Velden, C., S., Bedka, K., M., 2009. Identifying the uncertainty in determining satellite-derived atmospheric motion vector height attribution. J. Applied Meteorology and Climatology 2, 380–392.
- Weissmann, M., Folger, K., Lange, H., 2013. Height correction of atmospheric motion vectors using lidar observations. JAMC 52, 1868–1877.